

## **The expression of brown fat associated proteins in colorectal cancer and the relationship of uncoupling protein 1 with prognosis**

Abdo Alnabulsi<sup>1,2</sup>, Beatriz Cash<sup>2</sup>, Yehfang Hu<sup>3</sup>, Linda Silina<sup>4</sup>, Ayham Alnabulsi<sup>2</sup>, Graeme I Murray<sup>1</sup>

<sup>1</sup>Pathology, School of Medicine, Medical Sciences and Nutrition, University of Aberdeen, Aberdeen, AB25, 2ZD, UK, <sup>2</sup>Vertebrate Antibodies, Zoology Building, Tillydrone Avenue, Aberdeen, AB24 2TZ, UK, <sup>3</sup>Scottish Fish Immunology Research Centre, School of Biological Sciences, University of Aberdeen, Aberdeen, AB24 2TZ, UK. <sup>4</sup>School of Biological Sciences, University of Aberdeen, Aberdeen, AB24 2TZ, UK.

Address correspondence to: Professor Graeme I Murray  
Email [g.i.murray@abdn.ac.uk](mailto:g.i.murray@abdn.ac.uk)  
Phone: +44(0)1224 553794  
Fax: +44(0)1224 663002

Number of figure: 2  
Number of tables: 4  
Words count: 3959

**Running title:** UCP1 and prognosis in colorectal cancer.

**Keywords:** biomarker, colorectal cancer, mitochondria, prognosis, uncoupling protein 1.

**Article category:** Tumour Markers and Signatures.

**Abbreviations:** AKT: AKT serine/threonine kinase 1; ATP: adenosine triphosphate; BLAST: basic local alignment search; CI: confidence interval; CIDEA: cell-death-inducing DNA fragment factor 45-like effector A; ELISA: enzyme-linked immunosorbent assay; ELOVL3: elongation of very long fatty acids 3; ELOVL5: elongation of very long fatty acids 5; EMVI: extramural venous invasion; MLH1: mutL homolog 1; MMR: mismatch repair protein; MSH2: mutS homolog 2; UCP1: uncoupling protein 1.

### **Novelty and Impact:**

This is the first study to examine brown fat-associated proteins CIDEA, ELOVL3, ELOVL5 and UCP1 in colorectal cancer. Monoclonal antibodies towards these proteins were produced using specific peptide immunogens which had been identified using a range of bioinformatics tools. CIDEA, ELOVL3, ELOVL5 and UCP1 were evaluated in well-characterised discovery and validation cohorts of colorectal cancer. The expression of UCP1 emerged as a biomarker strongly and independently associated with survival in colorectal cancer.

**Abstract**

Colorectal carcinoma is one of the most common types of malignancy and a leading cause of cancer related death. The aberrant expression of a brown fat-like phenotype in cancer cells has been previously implicated in tumour growth. Therefore, the expression of brown fat-associated proteins in colorectal cancer could be associated with tumour prognosis.

Monoclonal antibodies to brown fat-associated proteins CIDEA, ELOVL3, ELOVL5, and UCP1 were developed. The antibodies were used to profile the expression of protein targets by immunohistochemistry in a discovery cohort comprising 50 normal colonic mucosa samples and 274 primary colorectal cancers and a validation cohort comprising 549 colorectal cancers.

Immunostaining for UCP1 was observed in the majority of colorectal tumours while no immunostaining was observed in normal colonic mucosa ( $p < 0.001$ ). The expression of UCP1 was significantly associated with better overall survival in both the discovery cohort (HR=0.615, 95%CI=0.416-0.909,  $\chi^2 = 6.119$ ,  $p = 0.013$ ) and the validation cohort (HR=0.629, 95%CI=0.480-0.825,  $\chi^2 = 11.558$ ,  $p = 0.001$ ). Furthermore, UCP1 was independently prognostic in multivariate analysis ( $p = 0.004$ ).

This study has identified the brown fat-like phenotype as a novel pathway associated with survival in colorectal cancer. The expression of UCP1 was identified as a significant prognostic biomarker for colorectal cancer.

## Introduction

Colorectal cancer is a common malignancy with a poor mortality rate and a negative impact on the quality of life of survivors.<sup>1,2</sup> The incidence rate of colorectal cancer is relatively high in the developed world and such figures are expected to continue rising in the future.<sup>3,4</sup> Although the mortality rate of colorectal cancer has been declining as result of the ongoing developments in clinical practice, the average five-year survival rate remains relatively poor at around 55%.<sup>2</sup> To improve our understanding of colorectal tumourigenesis and provide a platform for innovative improvements in the outcome from colorectal cancer, there is still a need for further molecular characterisation of colorectal cancer.<sup>5,6</sup>

Adipose tissue is a connective tissue that is mainly populated by adipocyte and pre-adipocyte cells. The vast majority of fat tissue in adult humans is classified as white fat and is involved in many functions such as energy storage, metabolism, insulin sensitivity and inflammation.<sup>7</sup> The other type of fat tissue is known as brown fat which is composed of brown adipocytes that are rich in mitochondrial content thus giving deposits of brown fat their characteristic brownish colour.<sup>7</sup> Brown fat is limited to very small depots in the cervical, supraclavicular, axillary and paravertebral areas in adult humans.<sup>8</sup> Brown fat has been primarily implicated in energy expenditure and in diseases such diabetes and obesity.<sup>7</sup>

The brown fat phenotype is primarily characterised by the expression of uncoupling protein 1 (UCP1). The expression of UCP1 causes a proton leak in the mitochondrial respiratory chain leading to energy dissipation as heat rather than in the form of adenosine triphosphate (ATP), therefore; it is mainly associated with energy expenditure and metabolism.<sup>9</sup> Other key proteins associated with brown fat phenotype include; cell-death-inducing DNA fragment factor 45-like effector A (CIDEA) and elongation of very long fatty acids 3 (ELOVL3).<sup>10,11</sup> The main biological function of CIDEA has not been fully defined but has been mainly implicated in lipid and energy metabolism.<sup>12</sup> ELOVL3 elongates

saturated and monounsaturated fatty acids and is involved in triglyceride formation in brown adipocytes.<sup>13</sup> Whereas, ELOVL5 is a novel family member of long fatty chain elongases and is involved in the elongation of polyunsaturated fatty acids such as arachidonic acid and docosahexaenoic acid.<sup>14</sup>

There has been limited research on the expression of brown fat-phenotype in neoplasms of epithelial origin. The manifestation of brown fat phenotype, characterised by UCP1 expression, was detected by immunohistochemistry in the epithelial compartment of prostate cancer tissue, and *in vitro* analysis showed this phenotype was associated with tumour growth and progression.<sup>15</sup> The expression of UCP1 was also detected in a subpopulation of cancer stem cells in the early stages of breast cancer xenografts.<sup>16</sup>

The potential expression of the brown fat phenotype in colorectal carcinoma is unknown and more importantly, the relationship between the expression of this phenotype and survival among other clinico-pathological parameters has not been investigated. Therefore, the aim of this study was to characterise the expression of key brown fat-associated proteins and to evaluate their clinical relevance in colorectal cancer.

Using monoclonal antibodies, we have developed to brown fat-associated proteins, we have evaluated the expression of CIDEA, ELOVL3, ELOVL5 and UCP1 on tissue microarrays containing well-characterised cohorts of primary colorectal cancers. The use of tissue microarrays is a well-established approach to high throughput immunohistochemistry-based biomarker studies. The expression profile of each protein was established by light microscopy using a semi-quantitative scoring system.<sup>17</sup> The prognostic significance of each protein was determined by assessing the relationship between their expression in tumours and overall survival.

## **Materials and methods**

### **Monoclonal antibody development**

Monoclonal antibodies to CIDEA, ELOVL3, ELOVL5 and UCP1 were developed using short synthetic peptides.<sup>17</sup> To facilitate the identification of specific immunogenic peptides (8-12 amino acids in length) a range of bioinformatics tools were used (Supplementary Table S1). This comprised homology and structural analysis of each protein and bioinformatics prediction of each immunogen peptide. Homology analysis was mainly performed by aligning the amino acids sequence of each protein with their family members, thereby, selecting specific peptides from regions with high amino acids diversity (Supplementary Figure S1). The secondary and tertiary structures of each protein were predicted using online bioinformatics tools and then analysed to identify accessible regions (Supplementary Figures S2, S3 and S4). Finally, after selecting a candidate peptide sequence, its specificity to the target of interest was evaluated by sequence comparison against UniProtKB 'Complete human proteome database' using basic local alignment search tool (BLAST).

The amino acid sequences of peptides used to generate the antibodies and their location on each protein are specified in Supplementary Table S2. All peptides (Almac Sciences Ltd, Edinburgh, UK) were conjugated to ovalbumin for immunisations and to bovine serum albumin for the enzyme-linked immunosorbent assay (ELISA) screenings.<sup>18</sup> The immunisation via the subcutaneous route, the production of hybridomas and the ELISA screenings were carried out as previously described.<sup>19-21</sup>

### **Monoclonal antibody characterisation**

To evaluate the specificity of monoclonal antibodies, immunoblotting was performed using whole cell lysate which is made of human embryonic kidney cells-HEK 293,

overexpressing the relevant protein as a positive control and lysates from HEK 293 cells containing empty vector as a negative control (Novus Biologicals, Oxfordshire, UK and OriGene Technologies Rockville, USA). To overexpress each protein, HEK293 cells had been transiently transfected using the full length reading frame cDNA plasmid of the corresponding gene (Novus Biologicals, Oxfordshire, UK and OriGene Technologies Rockville, USA). The immunoblotting was carried out as previously described.<sup>22</sup>

The initial immunohistochemical evaluation of each of the antibodies and their tissue specificity was performed using a multi-tissue microarray which was designed to include a wide range of normal tissue and tumour types (Supplementary Table S3).

### **Colorectal cancer patient cohorts**

Two well-characterised patient cohorts were used for profiling each brown fat associated protein in colorectal cancer. The patient cohorts were retrospectively acquired from the Grampian Biorepository ([www.biorepository.nhsgrampian.org](http://www.biorepository.nhsgrampian.org)) and randomly assigned to discovery and validation sets at a ratio of 1:2. Both groups of patients had undergone surgery with curative intent for primary colorectal cancers between 1994 and 2011, at Aberdeen Royal Infirmary-NHS Grampian (Aberdeen, UK). Only patients with UICC stage I, stage II or stage III were included in the study while patients with histological evidence of distant metastasis were excluded. Patients who had received neoadjuvant chemotherapy and/or radiotherapy were also excluded. All tissue samples were processed following a standard protocol. Further details on the histopathological processing of tissue specimens are described in Supplementary Materials and Methods S1.

Tissue samples from 274 patients were selected as the discovery cohort and 549 patients were selected as the validation cohort. The clinico-pathological characteristics of

patients in the discovery and validation cohorts were comparable descriptively and statistically, except for mismatch repair protein (MMR) status (Supplementary Table S4).

Survival data on a 6-monthly basis was updated from the NHS Grampian electronic patient management system. Overall survival time was defined as the period from 28 days after the date of surgery to the date of death from any cause. At the date of final censoring of patient outcome data (March 2012), no patients had been lost to follow-up and patients who were still alive were censored. The clinico-pathological characteristics and their association with survival for each patient cohort are described in Table 1.

For the discovery cohort, there had been 112 (40.9%) deaths, the median survival was 109 months (95% CI=84-134 months) and the median follow-up time, calculated by the “reverse Kaplan-Meier” method, was 61 months (95% CI=44-78 months). For the validation cohort, there had been 229 (41.7%) deaths, the median survival was 93 months (95% CI=74-112 months) and the median follow-up time was 70 months (95% CI=66-74 months).

The Royal College of Pathologists UK guidelines, including guidance from version 5 of the tumour, node, metastasis staging system, were followed for the histopathological reporting of resection specimens of colorectal cancer.<sup>23</sup>

### **Colorectal cancer tissue microarrays**

A colorectal cancer tissue microarray was constructed from the discovery cohort consisting of 274 primary colorectal tumours and 50 normal colon mucosal samples (acquired from at least 10 cm in distance from the tumour). Similarly, a tissue microarray was constructed consisting of 549 primary tumour samples from the validation cohort. For each tissue sample, two representative 1 mm cores were obtained from the corresponding formalin fixed, paraffin embedded block to construct the tissue microarrays.<sup>21,22,24</sup>

## **Immunohistochemistry**

### **Monoclonal antibody characterisation using multi-tissue microarray**

Immunohistochemistry was performed using a Dako autostainer (Dako universal staining system, Dako/Agilent Technologies LDA UK Limited, Cheadle, UK).<sup>21,22</sup> The immunohistochemistry method is detailed in Supplementary Materials and Methods S1. Antibody diluent (Dako) was used in place of the primary monoclonal antibody as a negative control. For each antibody one slide was tested without antigen retrieval and one slide was tested with antigen retrieval. Antigen retrieval was performed by microwaving the tissue slides for 20 minutes while fully immersed in 10mM citrate buffer pH 6.0. The immunostaining results were assessed using light microscopy by AA and GIM. The immunostaining profile for each antibody (i.e. the subcellular localisation, the tissue expression profile and the presence of any background staining) was assessed and interpreted in the context of existing knowledge for the tissue specific expression of each gene. The specificity of UCP1 was additionally assessed using hibernoma (brown fat tumour) samples.

### **Protein characterisation using colorectal cancer tissue microarrays**

The immunostaining of the colorectal cancer tissue microarrays was performed for each antibody as described above. An appropriate positive control tissue (CIDEA, ELOVL3 and ELOVL5-liver, UCP1-pancreas and hibernoma) was included for each antibody. The negative control for each antibody was antibody diluent in place of the primary monoclonal antibody. The immunostaining results were evaluated under light microscopy using an established semi-quantitative scoring system that is based on the intensity of immunostaining (Supplementary Figure S5).<sup>22,24-26</sup> Positive staining was regarded as any staining of tumour cells while negative staining was considered as an absence of tumour cell staining as previously described.<sup>22,24-26</sup> The scoring was conducted independently by two observers (AA



and GIM) who were unaware of the outcome. Any discrepancies in the scores were resolved through simultaneous re-evaluation of the cores by both observers. Cases were recorded as missing if the evaluation of immunostaining was not possible due to the tissue cores being damaged/folded during the staining process precluding immunohistochemical assessment or there were no tumour cells present in the relevant cores.

### **Assessment of mismatch repair protein (MMR) status**

The assessment of MLH1 and MSH2 proteins by immunohistochemistry was used to determine whether tumours were either MMR protein proficient or MMR protein deficient.<sup>21</sup>

### **Data analysis and statistics**

The immunostaining scores of the colorectal cancer tissue microarrays were recorded in an Excel 2013 spreadsheet before being analysed using IBM SPSS version 24 for Windows 7™ (IBM, Portsmouth, UK). Statistical tests that were used to analyse the data included Mann-Whitney U test, chi-squared test, Kaplan-Meier survival analysis, log-rank test and Cox regression analysis for the calculation of hazard ratios and 95% CIs. The clinico-pathological characteristics of both cohorts were compared descriptively and by chi-squared tests. Univariate survival analysis was performed for both the discovery and validation cohorts. For the validation cohort multivariate Cox regression analysis (“ENTER” method) was also used to evaluate the prognostic significance of each protein in relation to established prognostic variables: age, tumour differentiation, T category, N category and extramural venous invasion (EMVI). Patients were also dichotomised into clinically relevant low-risk and high-risk stratification groups based on T category, N category, tumour differentiation and EMVI: low-risk group: (pT1-pT3, EMVI absent (V0) and well/moderately differentiated tumour (G1, G2)) and pN0 vs high-risk group: (pT4 or

EMVI present (V1) or poorly differentiated tumour (G3)) and pN0 or any lymph node positive tumour (pN1 or pN2).<sup>27</sup> A probability value of  $p \leq 0.05$  was regarded as statistically significant. Additional details of the data analysis are provided in Supplementary Materials and Methods S1.

### **Ethics**

Ethical approval for the use of colorectal and other tissue samples was given by the Grampian Biorepository scientific access group committee (Tissue request No.0002). The use of tissue samples included in the tissue microarrays did not require written consent from patients.

## **Results**

### **Monoclonal antibody development**

During the hybridoma production, ELISA screenings were used to evaluate the specificity of antibodies to immunogen peptides used in immunisation. Further evaluation of the specificity of each antibody towards the relevant protein was performed by immunoblotting. A single band at the expected molecular weight of the relevant protein was observed in the corresponding overexpression lysate while no band was detected in the negative control (Supplementary Figure S6).

The immunoreactivity and tissue specificity of antibodies on a multi-tissue microarray was also evaluated by immunohistochemistry. Neat culture supernatant was used for each antibody except for ELOVL3 (1:10 dilution) and antigen retrieval was required for each antibody. CIDEA was mainly expressed in normal colon and normal breast tissue. ELOVL3 enzyme was strongly expressed in normal skin, breast, colon, liver, while ELOVL5 was widely expressed. Immunoreactivity for UCP1 was observed in endocrine pancreas and in hibernoma tissue (Supplementary Figure S7).

### **Immunostaining profile of proteins in colorectal cancer**

In the discovery cohort, CIDEA, ELVOL3 and ELVOL5 each showed immunoreactivity in normal colonic epithelium and primary colorectal tumours. There was no immunoreactivity for UCP1 in normal colonic mucosa while the majority of primary tumours showed immunostaining for UCP1. Furthermore, the expression profile of each protein in normal mucosa versus tumour tissues was analysed using Mann Whitney U test. There was a significant increase in the intensity of immunostaining of CIDEA ( $p<0.001$ ), ELOVL5 ( $p<0.001$ ) and UCP1 ( $p<0.001$ ) in primary tumour compared to normal colonic mucosa. Whereas a decrease in the expression of ELOVL3 ( $p=0.020$ ) was observed in

colorectal tumours compared to normal colorectal epithelium. The immunoreactivity for each protein was exclusively localised to the cell cytoplasm and no intra-tumour heterogeneity was observed (Supplementary Figure S8).

The frequency distribution of immunostaining intensities was also evaluated for each protein in the discovery and validation cohorts (Figure 1 and Table 2). The majority of tumour tissues showed moderate and strong CIDEA staining while only 11% and 16% of tumours in the discovery and validation cohort respectively were CIDEA negative. Similar expression profiles were observed for ELOVL3 and ELOVL5 as both showed moderate and strong staining in the majority of tumour samples. As for UCP1, the majority of tumours showed weak immunostaining in both cohorts, while 34% and 41% were negatively stained in the discovery set and the validation set respectively.

When comparing the expression profiles for each protein between the two cohorts, no significant difference was observed for CIDEA, ELOVL3 and UCP1 (Table 2). There was significant variation ( $\chi^2=12.868$ ,  $p=0.005$ ) in the expression profile of ELOVL5 between the discovery and validation cohorts and the main difference was between the proportion of moderate and strong immunostaining.

### **Relationship of brown fat protein expression with clinico-pathological parameters**

The relationships between the pathological parameters and the expression of each protein were evaluated in the discovery and the validation cohorts (Supplementary Table S5). CIDEA showed significant association only with lymph node stage in both the discovery and validation cohorts. The expression of ELOVL3 was significantly associated with MMR protein status, extramural venous invasion and UICC stage in both cohorts. The most robust relationships were observed in relation to UCP1 which was significantly associated with tumour stage, lymph node stage, UICC stage and overall risk group in each cohort

(Supplementary Tables S5 and S6). The expression of UCP1 significantly decreased as tumour stage increased from stage I to stage III (Supplementary Figure S9).

## Survival analysis

### Discovery cohort

Different cut-off points of the immunostaining scores were used to investigate the association between the expression of protein targets and overall survival in the discovery cohort. Significant associations were observed between overall survival and the expression of CIDEA and UCP1 (Table 3).

UCP1 showed the most significant and robust association with survival following the dichotomisation of UCP1 staining categories into positive *versus* negative staining (Figure 2). Expression of UCP1 was significantly associated with better survival (HR=0.615, 95%CI=0.416-0.909,  $\chi^2=6.119$ ,  $p=0.013$ ). Patients with tumours not expressing UCP1 (n=90) had a poorer survival with a median survival of 110 months (95%CI=26-193 months) compared to a median survival of 114 months (95%CI=95-132 months) for patients with tumours expressing UCP1 (n=174).

The expression of CIDEA was significantly associated with survival when CIDEA expression was compared to absent CIDEA expression (HR=0.286, 95%CI=0.138-0.593,  $\chi^2=12.945$ ,  $p<0.001$ ; Supplementary Figure S10).

There was no significant association between ELOVL3 or ELOVL5 and survival in the discovery cohort (Table 3).

### Validation cohort

Consistent with the result in the discovery cohort, there was also a significant association between UCP1 and survival (HR=0.629, 95%CI=0.480-0.825,  $\chi^2=11.558$ ,

$p=0.001$ ; Figure 2). Patients with tumours not expressing UCP1 ( $n=214$ ) had a poorer survival with a median survival of 75 months (95%CI=65-85 months) compared to a median survival of 131 months (95%CI undefined) for patients with tumours expressing UCP1 ( $n=303$ ).

Multivariate analysis was also performed in the validation cohort to determine whether UCP1 was prognostically independent of clinically established parameters (Table 4 and Supplementary Table S7). The expression of UCP1, stratified as negative *versus* positive, was significantly associated with survival independent of the main prognostic factors. Multivariate analysis was also performed to determine whether UCP1 was prognostically independent of parameters that would be available at the time of biopsy (Supplementary Table S8). This analysis showed that the expression of UCP1 was also strongly prognostic in a scenario where only pre-surgical resection parameters are available ( $p=0.001$ ).

There was no significant association between the expression of CIDEA and survival in the validation cohort.

## Discussion

Colorectal cancer is a common type of cancer and one of the major contributors to cancer-related mortalities.<sup>1,2</sup> The survival rate of colorectal cancer patients is still relatively poor despite recent advances in understating the molecular pathology of this type of tumour.<sup>2</sup> Better understanding of novel molecular pathways underpinning colorectal cancer progression is necessary to improve the current survival rates.

The expression of brown fat phenotype has been observed in prostate, lung and breast carcinoma and has been implicated in tumour growth.<sup>15,16,28</sup> However, the expression of this phenotype in colorectal carcinoma and its association with survival among other clinico-pathological parameters has not yet been investigated.

In this study, a peptide immunogen approach was used to develop a panel of monoclonal antibodies to brown fat-associated proteins CIDEA and ELOVL3, ELOVL5 and UCP1. The antibodies were validated by immunoblotting and then their immunoreactivity was evaluated by immunohistochemistry on a multi-tissue microarray. The immunostaining profiles of CIDEA, ELOVL3 and ELOVL5 in the multi-tissue microarray were consistent with the knowledge on the mRNA expression of these genes.<sup>29,30</sup> The expression of UCP1 in normal endocrine pancreas<sup>31</sup> and hibernoma<sup>32</sup> was also in agreement with the current limited knowledge of the expression of this protein.

After validating the antibodies on the multi-tissue microarray, they were used to profile the expression pattern of each protein on well-characterised discovery and validation cohorts of colorectal cancers. Statistical and descriptive analysis of the clinico-pathological characteristics of patients and their association with survival showed that both cohorts were comparable and valid for the purpose of this study.

The results showed that there was a significant increase in the expression of brown fat-associated proteins CIDEA, ELOVL5 and UCP1 in colorectal tumour compared to normal

colonic mucosa. The detection of brown fat-like phenotype, characterised by UCP1 expression, in colorectal cancer could be the result of the unlimited plasticity of cancer stem cells, which can differentiate into multiple lineages with various phenotypes based on genetic mutations and microenvironmental factors.<sup>15,16</sup> The origin of cancer stem cells could be normal stem cells, resident in the colonic crypts or recruited from bone marrow by inflammatory mediators, that may have been transformed as a result of oncogenic mutations.<sup>33,34</sup> Cancer stem cells could also originate from normal epithelial cells as a result of epithelial-mesenchymal transition which is a process implicated in colorectal cancer.<sup>35</sup>

The prognostic value of each protein was firstly assessed by investigating associations between the expression of proteins and overall survival in the discovery cohort, and then the results were confirmed in the validation cohort. This revealed there was a significant association between the expression of UCP1 and better survival in colorectal cancer in both the discovery and validation cohorts. Using a robust cut-off point (positive *versus* negative), a considerable difference in median survival (56 months) was observed between the poor prognosis group (i.e. patients with tumours not expressing UCP1) and the good prognosis patient group (i.e. patients with tumours expressing UCP1). More importantly, the prognostic impact of UCP1 was significantly independent of established prognostic parameters. Therefore, the assessment of UCP1 by immunohistochemistry could be a valuable addition to current prognostic parameters in clinical practice as positive UCP1 immunostaining *versus* negative is a robust cut-off point which could be evaluated by straightforward immunohistochemical analysis on fixed tumour tissue. However, potential limitations of this study are the size of the discovery cohort and the reliance on one technology for validation (i.e. immunohistochemistry). In addition, there is still a need for additional validation of the prognostic impact of UCP1. It may also be worthwhile evaluating UCP1 in serum samples



from CRC patients. More importantly, the biology of UCP1 and associated pathways need to be investigated in relation to cancer development and growth.

The expression of UCP1 was also independently prognostic in multivariate analysis using parameters that would be available at the biopsy stage. Therefore, UCP1 could also be a useful biopsy-biomarker since it would provide prognostic information at an early stage prior to tumour resection. This is particularly relevant as neoadjuvant therapy followed by active surveillance is a treatment strategy which is likely to be increasingly used.<sup>36</sup>

The positive impact of UCP1 on survival may be explained by the role of UCP1 in the mitochondrion. Functional mitochondria is essential for metabolism, oxidative stress, apoptosis, signalling and proliferation.<sup>37</sup> Overexpressing UCP1 in breast cancer cells line resulted in mitochondrial dysfunction that lead to a significant reduction in tumour growth.<sup>38</sup> Tumour growth was inhibited by mitochondrial-induced catabolism in cancer cells expressing UCP1.<sup>38</sup>

In another study, the overexpression of uncoupling protein 3, a close family member of UCP1, reduced the growth of skin cancer in mice as a result of constitutive oxidation of substrates and nutrients that are essential for maintaining tumour growth, without simultaneous ATP production.<sup>39</sup> Furthermore, mitochondrial uncoupling blocked the activation of AKT serine/threonine kinase 1 (AKT) in mice thereby limiting proliferation and tumorigenesis.<sup>39</sup> Therefore, UCP1 could inhibit tumour growth by modulating and disrupting the metabolism of mitochondrion, which would lead to loss of nutrients, catabolism, disturbance of the cellular membrane and AKT inhibition (Supplementary Figure S11). Dysregulated energy metabolism has been accepted as a hallmark of carcinogenesis, where tumour cells manipulate different metabolic pathways to sustain their growth.<sup>40</sup> This could also be consistent with the consensus molecular subtype 3 (CMS3) of colorectal cancer where

multiple metabolic pathways are prominent.<sup>41</sup> However, there is still a need to evaluate the impact of UCP1 expression on mitochondrial metabolism in colorectal adenocarcinoma.

Another previous study by Zhau *et al*<sup>15</sup> also showed that proliferation was slower and apoptosis was higher in a prostate cancer cell line as a result of differentiation of cancer stem cells to cancer cells expressing UCP1. The expression of UCP1 might be associated with the differentiation of cancer stem cells to mature cancer cells that are more vulnerable to apoptosis.<sup>15</sup>

However, Singh and co-workers reported that tumour development and growth might be improved by the expression of UCP1 in a xenograft model of breast cancer.<sup>16</sup> The development of xenograft was inhibited after injecting mice with UCP1-negative cancer cells. Therefore, further investigation of the impact of UCP1 on tumour development and growth is still required.

In summary, this study has shown that UCP1, which is normally not present in normal colonic mucosa, is expressed in colorectal cancer and is significantly and independently associated with survival. This means the assessment of UCP1 in colorectal cancer could be a useful addition to current prognostic parameters used in clinical practice. Furthermore, UCP1 is an actionable protein and therefore is a valid target for therapeutic intervention.

## **Funding**

Innovate UK, NHS Grampian endowment funds and Vertebrate Antibodies Ltd.

**Conflict of interests**

Abdo Alnabulsi was a PhD student funded by Vertebrate Antibodies Ltd and is now a knowledge transfer partnership (KTP) associate funded by Innovate UK and Vertebrate Antibodies Ltd. Beatriz Cash and Ayham Alnabulsi are employees of Vertebrate Antibodies. Graeme Murray is a scientific advisor to Vertebrate Antibodies. Yehfang Hu and Linda Silina declare no conflict of interest.

**Acknowledgements**

The immunohistochemistry was performed with the support of the Grampian Biorepository ([www.biorepository.nhsgrampian.org/](http://www.biorepository.nhsgrampian.org/)). The antibodies were developed in collaboration with Vertebrate Antibodies Ltd ([www.vertebrateantibodies.com](http://www.vertebrateantibodies.com)) from whom they are now available commercially.

## References

1. Marshall DC, Webb TE, Hall RA, Saliccioli JD, Ali R, Maruthappu M. Trends in UK regional cancer mortality 1991–2007. *Br J Cancer* 2016; **114**: 340-347.
2. Siegel RL, Miller KD, Fedewa SA, Ahnen DJ, Meester RG, Barzi A, Jemal A. Colorectal cancer statistics, 2017. *CA Cancer J Clin* 2017; **67**: 177-193.
3. Arnold M, Sierra MS, Laversanne M, Soerjomataram I, Jemal A, Bray F. Global patterns and trends in colorectal cancer incidence and mortality. *Gut* 2017; **66**: 683-691.
4. Ferlay J, Colombet M, Soerjomataram I, Dyba T, Randi G, Bettio M, Gavin A, Visser O, Bray F. Cancer incidence and mortality patterns in europe: Estimates for 40 countries and 25 major cancers in 2018. *Eur J Cancer* 2018; **103**: 356-387.
5. Alnabulsi A, Murray GI. Integrative analysis of the colorectal cancer proteome: potential clinical impact. *Expert Rev Proteomics* 2016; **13**: 917-927.
6. Alnabulsi A, Murray GI. Proteomics for early detection of colorectal cancer: recent updates. *Expert Rev Proteomics* 2018; **15**: 55-63.
7. Lehnig AC, Stanford KI. Exercise-induced adaptations to white and brown adipose tissue. *J Exp Biol* 2018; **221**: jeb161570.
8. Kim SH, Plutzky J. Brown fat and browning for the treatment of obesity and related metabolic disorders. *Diabetes Metab J* 2016; **40**: 12-21.
9. Jastroch M, Oelkrug R, Keipert S. Insights into brown adipose tissue evolution and function from non-model organisms. *J Exp Biol* 2018; **221**: jeb169425.

10. Wolf G. Brown adipose tissue: the molecular mechanism of its formation. *Nutr Rev* 2009; **67**: 167-171.
11. Fischer AW, Shabalina IG, Mattsson CL, Abreu-Vieira G, Cannon B, Nedergaard J, Petrovic N. UCP1 inhibition in cidea-overexpressing mice is physiologically counteracted by brown adipose tissue hyperrecruitment. *Am J Physiol Endocrinol Metab* 2017; **312**: E72-E87.
12. Abreu-Vieira G, Fischer AW, Mattsson C, de Jong JM, Shabalina IG, Ryden M, Laurencikiene J, Arner P, Cannon B, Nedergaard J, Petrovic N. Cidea improves the metabolic profile through expansion of adipose tissue. *Nat Commun* 2015; **6**: 7433.
13. Ji L, Gupta M, Feldman BJ. Vitamin D regulates fatty acid composition in subcutaneous adipose tissue through Elovl3. *Endocrinology* 2016; **157**: 91-97.
14. Wang Y, Torres-Gonzalez M, Tripathy S, Botolin D, Christian B, Jump DB. Elevated hepatic fatty acid elongase-5 activity affects multiple pathways controlling hepatic lipid and carbohydrate composition. *J Lipid Res* 2008; **49**: 1538-1552.
15. Zhau HE, He H, Wang CY, Zayzafoon M, Morrissey C, Vessella RL, Marshall FF, Chung LW, Wang R. Human prostate cancer harbors the stem cell properties of bone marrow mesenchymal stem cells. *Clin Cancer Res* 2011; **17**: 2159-2169.
16. Singh R, Parveen M, Basgen JM, Fazel S, Meshesha MF, Thames EC, Moore B, Martinez L, Howard CB, Vergnes L, Reue K, Pervin S. Increased expression of beige/brown adipose markers from host and breast cancer cells influence xenograft formation in mice. *Mol Cancer Res* 2016; **14**: 78-92.

17. Alnabulsi A, Swan R, Cash B, Alnabulsi A, Murray GI. The differential expression of omega-3 and omega-6 fatty acid metabolising enzymes in colorectal cancer and its prognostic significance. *Br J Cancer* 2017; **116**: 1612-1620.
18. Duncan ME, McAleese SM, Booth NA, Melvin WT, Fothergill JE. A simple enzyme-linked immunosorbent assay (ELISA) for the neuron-specific gamma isozyme of human enolase (NSE) using monoclonal antibodies raised against synthetic peptides corresponding to isozyme sequence differences. *J Immunol Methods* 1992; **151**: 227-236.
19. Murray GI, Duncan ME, Arbuckle E, Melvin WT, Fothergill JE. Matrix metalloproteinases and their inhibitors in gastric cancer. *Gut* 1998; **43**: 791-797.
20. Murray GI, Duncan ME, O'Neil P, Melvin WT, Fothergill JE. Matrix metalloproteinase-1 is associated with poor prognosis in colorectal cancer. *Nat Med* 1996; **2**: 461-462.
21. Brown GT, Cash BG, Blihoghe D, Johansson P, Alnabulsi A, Murray GI. The expression and prognostic significance of retinoic acid metabolising enzymes in colorectal cancer. *PLoS One* 2014; **9**: e90776.
22. Swan R, Alnabulsi A, Cash B, Alnabulsi A, Murray GI. Characterisation of the oxysterol metabolising enzyme pathway in mismatch repair proficient and deficient colorectal cancer. *Oncotarget* 2016; **7**: 46509-46527.
23. Williams GT, Quirke P, Shepherd NA. Dataset for colorectal cancer, 2nd ed. The Royal College of Pathologists, 2007, 1-27.
24. O'Dwyer D, Ralton LD, O'Shea A, Murray GI. The proteomics of colorectal cancer: Identification of a protein signature associated with prognosis. *PloS one* 2011; **6**:e27718.

25. Kumarakulasingham M, Rooney PH, Dundas SR, Telfer C, Melvin WT, Curran S, Murray GI. Cytochrome P450 profile of colorectal cancer: identification of markers of prognosis. *Clin Cancer Res* 2005; **11**: 3758-3765.
26. Brown GT, Cash B, Alnabulsi A, Samuel LM, Murray GI. The expression and prognostic significance of bcl-2-associated transcription factor 1 in rectal cancer following neoadjuvant therapy. *Histopathology* 2016; **68**: 556-566.
27. Pages F, Mlecnik B, Marliot F, Bindea G, Ou FS, Bifulco C, Lugli A, Zlobec I, Rau TT, Berger MD, Nagtegaal ID, Vink-Börger E, Hartmann A, Geppert C, Kolwelter J, Merkel S, Grützmann R, Van den Eynde M, Jouret-Mourin A, Kartheuser A, Léonard D, Remue C, Wang JY, Bavi P, Roehrl MHA, Ohashi PS, Nguyen LT, Han S, MacGregor HL, Hafezi-Bakhtiari S, Wouters BG, Masucci GV, Andersson EK, Zavadova E, Vocka M, Spacek J, Petruzela L, Konopasek B, Dunder P, Skalova H, Nemejcova K, Botti G, Tatangelo F, Delrio P, Ciliberto G, Maio M, Laghi L, Grizzi F, Fredriksen T, Buttard B, Angelova M, Vasaturo A, Maby P, Church SE, Angell HK, Lafontaine L, Bruni D, El Sissy C, Haicheur N, Kirilovsky A, Berger A, Lagorce C, Meyers JP, Paustian C, Feng Z, Ballesteros-Merino C, Dijkstra J, van de Water C, van Lent-van Vliet S, Knijn N, Muşină AM, Scripcariu DV, Popivanova B, Xu M, Fujita T, Hazama S, Suzuki N, Nagano H, Okuno K, Torigoe T, Sato N, Furuhashi T, Takemasa I, Itoh K, Patel PS, Vora HH, Shah B, Patel JB, Rajvik KN, Pandya SJ, Shukla SN, Wang Y, Zhang G, Kawakami Y, Marincola FM, Ascierto PA, Sargent DJ, Fox BA, Galon J. International validation of the consensus immunoscore for the classification of colon cancer: a prognostic and accuracy study. *Lancet* 2018; **391**: 2128-2139.
28. Giatromanolaki A, Balaska K, Kalamida D, Kakouratos C, Sivridis E, Koukourakis MI. Thermogenic protein UCP1 and UCP3 expression in non-small cell lung cancer: relation with glycolysis and anaerobic metabolism. *Cancer Biol Med* 2017; **14**: 396-404.

29. Westerberg R, Mansson JE, Golozoubova V, Shabalina IG, Backlund EC, Tvrdik P, Retterstøl K, Capecchi MR, Jacobsson A. ELOVL3 is an important component for early onset of lipid recruitment in brown adipose tissue. *J Biol Chem* 2006; **281**: 4958-4968.
30. Expression Atlas-The EMBL-European Bioinformatics Institute. Exploring gene expression results across species under different biological conditions.  
<https://www.ebi.ac.uk/gxa/home> (2018).
31. Sale MM, Hsu FC, Palmer ND, Gordon CJ, Keene KL, Borgerink HM, Sharma AJ, Bergman RN, Taylor KD, Saad MF, Norris JM. The uncoupling protein 1 gene, UCP1, is expressed in mammalian islet cells and associated with acute insulin response to glucose in african american families from the IRAS family study. *BMC Endocr Disord* 2007; **7**: 1.
32. Vijgen GH, Bouvy ND, Smidt M, Kooreman L, Schaart G, van Marken Lichtenbelt W. Hibernoma with metabolic impact? *BMJ Case Rep* 2012. doi:10.1136/bcr-2012-006325.
33. Puglisi MA, Tesori V, Lattanzi W, Gasbarrini GB, Gasbarrini A. Colon cancer stem cells: Controversies and perspectives. *World J Gastroenterol* 2013; **19**: 2997-3006.
34. Zeuner A, Todaro M, Stassi G, De Maria R. Colorectal cancer stem cells: from the crypt to the clinic. *Cell Stem Cell* 2014; **15**: 692-705.
35. Garza-Trevino EN, Said-Fernandez SL, Martinez-Rodriguez HG. Understanding the colon cancer stem cells and perspectives on treatment. *Cancer Cell Int* 2015; **15**: 2.
36. Chang H, Yu X, Xiao W, Wang Q, Zhou W, Zeng Z, Ding PR1, Li LR, Gao YH. Neoadjuvant chemoradiotherapy followed by surgery in patients with unresectable locally advanced colon cancer: a prospective observational study. *Onco Targets Ther* 2018; **11**:409-418.



37. Vyas S, Zaganjor E, Haigis MC. Mitochondria and cancer. *Cell* 2016; **166**: 555-566.
38. Sanchez-Alvarez R, Martinez-Outschoorn UE, Lamb R, Hult J, Howell A, Gandara R, Sartini M, Rubin E, Lisanti MP, Sotgia F. Mitochondrial dysfunction in breast cancer cells prevents tumor growth: understanding chemoprevention with metformin. *Cell Cycle* 2013; **12**: 172-182.
39. Nowinski SM, Solmonson A, Rundhaug JE, Rho O, Cho J, Lago CU, Riley CL, Lee S, Kohno S, Dao CK, Nikawa T, Bratton SB, Wright CW, Fischer SM, DiGiovanni J, Mills EM. Mitochondrial uncoupling links lipid catabolism to akt inhibition and resistance to tumorigenesis. *Nat Commun* 2015; **6**: 8137.
40. Hanahan D, Weinberg RA. Hallmarks of cancer: the next generation. *Cell* 2011; **144**: 646-674.
41. Guinney J, Dienstmann R, Wang X, De Reyniès A, Schlicker A, Soneson C, Marisa L, Roepman P, Nyamundanda G, Angelino P, Bot BM, Morris JS, Simon IM, Gerster S, Fessler E, De Sousa E Melo F, Missiaglia E, Ramay H, Barras D, Homicsko K, Maru D, Manyam GC, Broom B, Boige V, Perez-Villamil B, Laderas T, Salazar R, Gray JW, Hanahan D, Tabernero J, Bernards R, Friend SH, Laurent-Puig P, Medema JP, Sadanandam A, Wessels L, Delorenzi M7, Kopetz S, Vermeulen L, Tejpar S. The consensus molecular subtypes of colorectal cancer. *Nat Med* 2015; **21**: 1350-1356.

**Table 1. Clinico-pathological characteristics of all patients, their tumours and the relationship of each variable with overall survival in the discovery and validation cohorts.**

Clinico-pathological characteristic		Discovery cohort (n=274)		Validation cohort (n=549)	
		Percentage (number)	Relationship with survival	Percentage (number)	Relationship with survival
Gender	Male	52.9 (145)	$\chi^2=0.137$ , $p=0.711$	51.9 (285)	$\chi^2=0.000$ , $p=0.989$
	Female	47.1 (129)		48.1 (264)	
Age	<70	43.4 (119)	$\chi^2=3.045$ , $p=0.065$	45.5 (249)	$\chi^2=26.095$ , <b><math>p&lt;0.001</math></b>
	$\geq 70$	56.6 (155)		54.6 (300)	
Bowel screening programme detected	Yes	12 (33)	$\chi^2=10.520$ , <b><math>p=0.001</math></b>	9.1 (50)	$\chi^2=6.721$ , <b><math>p=0.010</math></b>
	No	88 (241)		90.9 (499)	
Tumour site	Proximal colon	34.3 (94)	Proximal vs distal, $\chi^2=3.040$ , $p=0.081$	40.2 (221)	Proximal vs distal, $\chi^2=6.392$ , <b><math>p=0.011</math></b>
	Distal colon	46 (126)	Distal vs rectal, $\chi^2=0.003$ , $p=0.953$	40.7 (223)	Distal vs rectal, $\chi^2=1.075$ , $p=0.300$
	Rectum	19.7 (54)	Colon vs rectum, $\chi^2=0.586$ , $p=0.444$	19.1 (105)	Colon vs rectum, $\chi^2=0.002$ , $p=0.692$
Tumour differentiation	G1/G2, well/moderate	90.9 (249)	$\chi^2=1.932$ , $p=0.165$	92.3 (507)	$\chi^2=1.149$ , $p=0.284$
	G3, poor	9.1 (25)		7.7 (42)	
Extramural venous invasion	V1, present	23.4 (64)	$\chi^2=62.876$ , <b><math>p&lt;0.001</math></b>	20.4 (112)	$\chi^2=61.508$ , <b><math>p&lt;0.001</math></b>
	V0, absent	76.6 (210)		79.6 (437)	
Mismatch repair protein status	Deficient	23.1 (62)	$\chi^2=0.402$ , $p=0.526$	12.7 (68)	$\chi^2=2.933$ , $p=0.087$
	Proficient	76.9 (206)		87.3 (468)	
pT category	pT1	5.8 (16)	pT1 vs pT2, $\chi^2=1.990$ , $p=0.158$	4.5 (25)	pT1 vs pT2, $\chi^2=1.176$ , $p=0.278$
	pT2	12.8 (35)	pT2 vs pT3, $\chi^2=6.950$ , <b><math>p=0.008</math></b>	17.5 (96)	pT2 vs pT3, $\chi^2=16.205$ , <b><math>p&lt;0.001</math></b>
	pT3	63.5 (174)	pT3 vs pT4, $\chi^2=33.960$ , <b><math>p&lt;0.001</math></b>	63.9 (351)	pT3 vs pT4, $\chi^2=14.681$ , <b><math>p&lt;0.001</math></b>
	pT4	17.9 (49)		14.1 (77)	
pN category	pN0	58 (159)	pN0 vs pN1, $\chi^2=25.234$ , <b><math>p&lt;0.001</math></b>	58 (320)	pN0 vs pN1, $\chi^2=35.321$ , <b><math>p&lt;0.001</math></b>
	pN1	26 (70)	pN1 vs pN2, $\chi^2=10.984$ , <b><math>p=0.001</math></b>	26 (141)	pN1 vs pN2, $\chi^2=11.300$ , <b><math>p=0.001</math></b>
	pN2	16 (45)		16 (88)	
UICC stage	I	16.4 (45)	I vs II, $\chi^2=3.599$ , $p=0.058$	18.2 (100)	I vs II, $\chi^2=3.269$ , $p=0.071$
	II	41.6 (114)	II vs III, $\chi^2=35.045$ , <b><math>p&lt;0.001</math></b>	40.1 (220)	II vs III, $\chi^2=45.613$ , <b><math>p&lt;0.001</math></b>
	III	42 (115)		41.7 (229)	
Low risk* vs high risk	Low risk	46.4 (127)	Low risk vs high risk, $\chi^2=45.973$ , <b><math>p&lt;0.001</math></b>	45.5 (250)	Low risk vs high risk, $\chi^2=60.249$ , <b><math>p&lt;0.001</math></b>
	High risk	53.6 (147)		54.5 (299)	

Significant values are highlighted in bold. \*Low risk (pT1-pT3 and G1 or G2 and V0, pN0): high risk (pT4 or G3 or V1 and pN0 or any pN1 or pN2 tumour)

**Table 2. Comparison of the expression profile of each protein in tumour samples in the discovery and the validation cohorts.**

Expression category	CIDEA		ELOVL3		ELOVL5		UCP1	
	Discovery	Validation	Discovery	Validation	Discovery	Validation	Discovery	Validation
Negative	11 (4%)	16 (3%)	22 (8%)	28 (5%)	10 (4%)	17 (3%)	90 (34%)	214 (41%)
Weak	42 (16%)	107 (21%)	50 (19%)	117 (22%)	53 (20%)	111 (21%)	129 (49%)	229 (44%)
Moderate	81 (32%)	171(33%)	83 (32%)	141 (26%)	73 (28%)	206 (39%)	32 (12%)	54 (11%)
Strong	124 (48%)	222 (43%)	108 (41%)	249 (47%)	128 (48%)	193 (37%)	13 (5%)	20 (4%)
Chi-squared test: discovery vs validation	$\chi^2=3.579$ , p=0.311		$\chi^2=6.331$ , p=0.097		$\chi^2=12.868$ , <b>p=0.005</b>		$\chi^2=4.097$ , p=0.251	

**Table 3. The relationship between the expression of each protein and survival in the discovery cohort using different cut-off points for the intensity of the immunostaining.**

<b>CIDEA (n=258)</b>	Negative=11 (4%) Weak=42 (16%) Moderate=81 (32%) Strong=124 (48%)	Negative=11 (4%) Weak/moderate /strong= 247 (96%)	Negative/weak=53 (20%) Moderate/strong=205 (80%)	Strong=134 (48%) Negative/weak/moderate=124 (52%)
	$\chi^2=13.385$ , p= <b>0.004</b>	$\chi^2=12.945$ , p= <b>0.001</b>	$\chi^2=0.095$ , p=0.582	$\chi^2=0.193$ , p=0.660
<b>ELOVL3 (n=263)</b>	Negative=22 (8%) Weak= 50 (19%) Moderate=83 (32%) Strong=108 (41%)	Negative=22 (8%) Weak/moderate/strong=241 (92%)	Negative/weak=72 (27%) Moderate/strong=191 (73%)	Strong=108 (41%) Negative/weak/moderate=155 (59%)
	$\chi^2=5.289$ , p=0.152	$\chi^2=2.101$ , p=0.147	$\chi^2=3.313$ , p=0.069	$\chi^2=3.787$ , p=0.052
<b>ELVOL5 (n=264)</b>	Negative=10 (4%) Weak=53 (20%) Moderate=73 (28%) Strong=128 (48%)	Negative=10 (4%) Weak/moderate/strong=254 (96%)	Negative/weak=63 (24%) Moderate/strong=201 (76%)	Strong=128 (48%) Negative/weak/moderate=136 (52%)
	$\chi^2=3.571$ , p=0.312	$\chi^2=0.751$ , p=0.386	$\chi^2=0.913$ , p=0.339	$\chi^2=0.094$ , p=0.759
<b>UCP1 (n=264)</b>	Negative=90 (34%) Weak=129 (49%) Moderate=32 (12%) Strong=13 (5%)	Negative=90 (34%) Weak/moderate/strong=174 (66%)	Negative/weak=219 (83%) Moderate/strong=45 (17%)	Strong=13 (5%) Negative/weak/moderate=251 (95%)
	$\chi^2=8.008$ , p= <b>0.046</b>	$\chi^2=6.119$ , p= <b>0.013</b>	$\chi^2=3.216$ , p=0.073	$\chi^2=0.000$ , p=0.996

Significant values are highlighted in bold.

**Table 4. Multivariate analysis of UCPI, age and risk groups in the validation cohort.**

Variable		Number of deaths/number of patients	Wald value	p-value	Hazard ratio (95%CI)
Age at surgery (< 70* vs ≥ 70)	< 70	79/249	25.184	< <b>0.001</b>	2.075 (1.560-2.760)
	≥ 70	150/300			
Low risk* vs high risk	Low risk	69/250	46.247	< <b>0.001</b>	2.773 (2.067-3.721)
	High risk	160/299			
UCPI (negative* vs positive)	Negative	101/214	8.385	<b>0.004</b>	0.669 (0.509-0.878)
	Positive	112/303			

Significant values are highlighted in bold. \*represents the reference group.

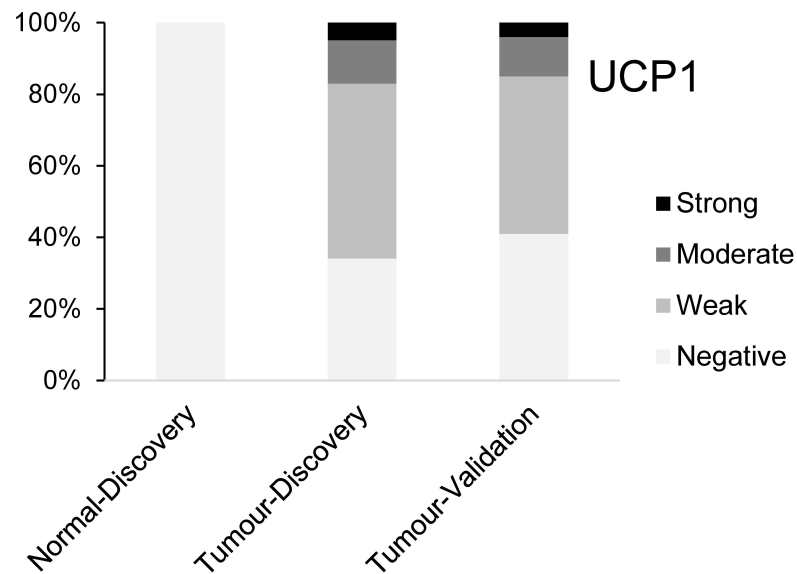
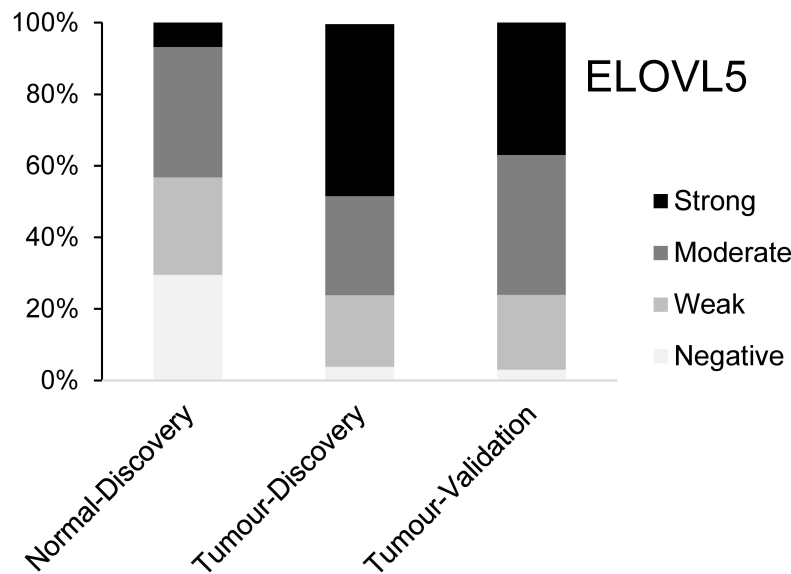
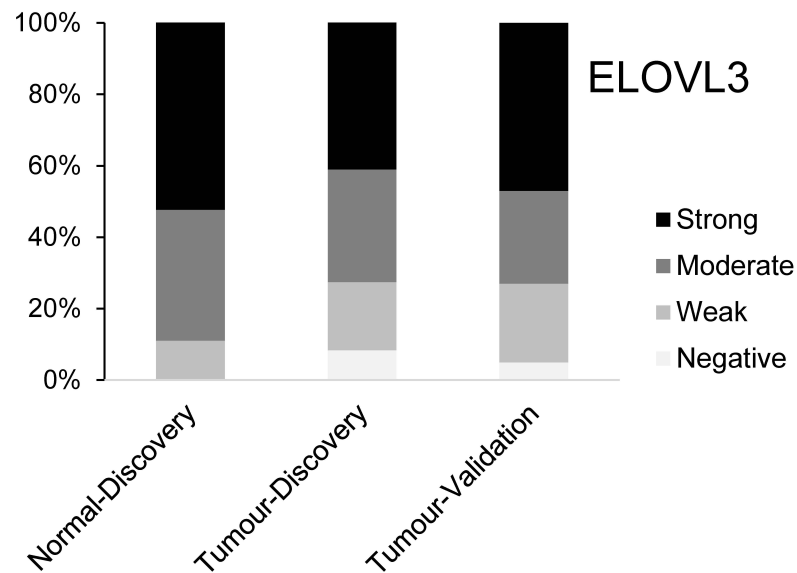
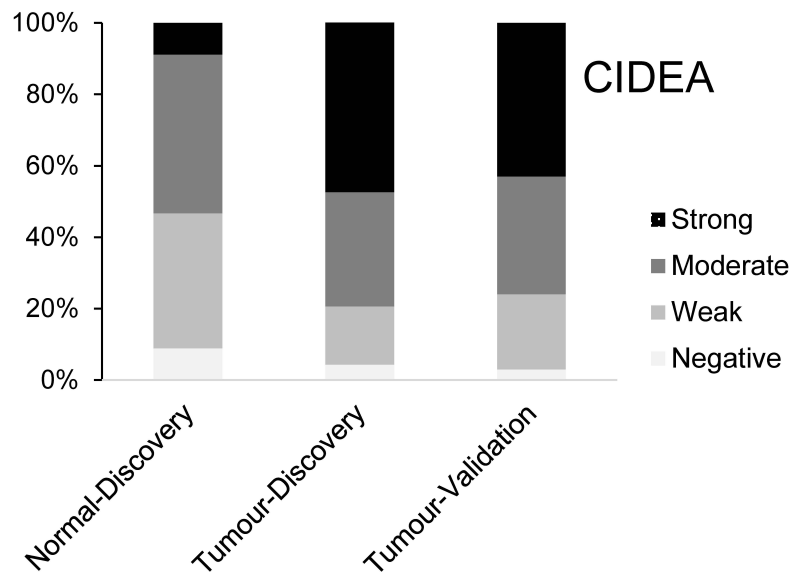
## Figure legends

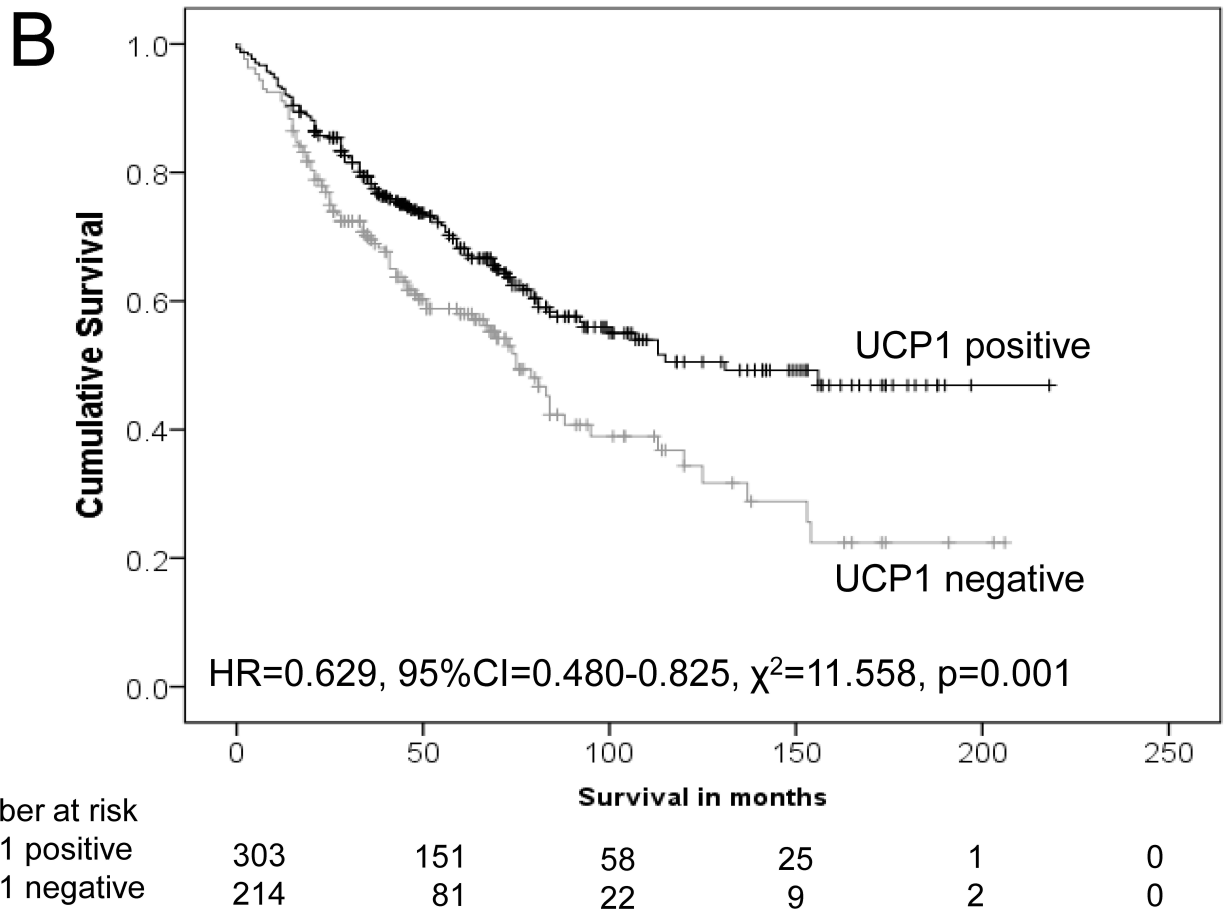
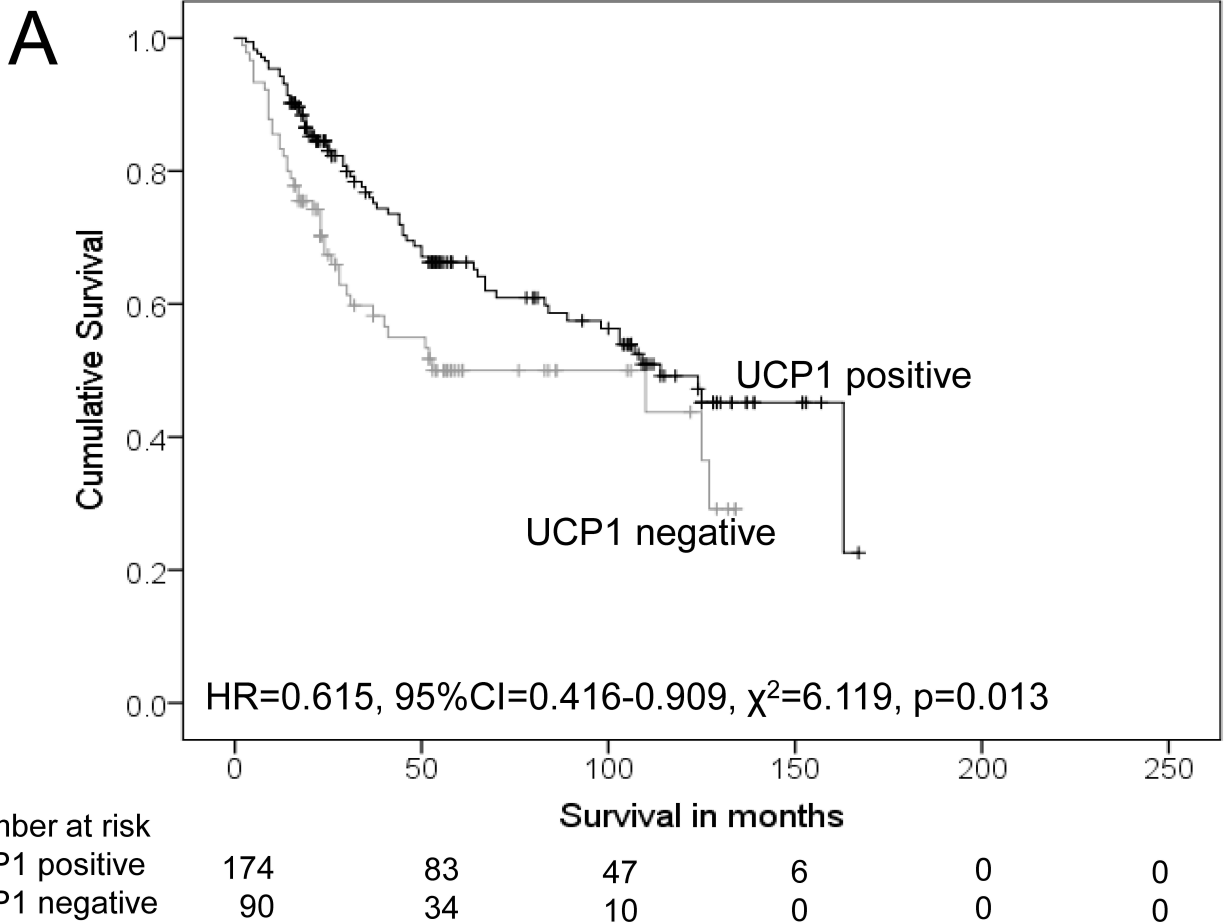
### Figure 1.

The frequency of negative, weak, moderate and strong immunostaining for CIDEA, ELOVL3, ELOVL5 and UCP1 in normal colonic mucosa and colorectal cancers in the discovery cohort and in colorectal cancers in the validation cohort.

### Figure 2.

The relationship between the expression of UCP1 and overall survival in the discovery cohort (A) and in the validation cohort (B) using positive expression *vs* negative expression as the cut-off point.







## **The expression of brown fat associated proteins in colorectal cancer and the relationship of uncoupling protein 1 with prognosis**

Abdo Alnabulsi, Beatriz Cash, Yehfang Hu, Linda Silina, Ayham Alnabulsi, Graeme I Murray

### **Supplementary Information**

#### **Materials and methods S1**

##### **Histopathological processing of colorectal tissue specimens**

Resection specimens were received fresh, opened along the anti-mesenteric aspect, excluding dissection through the tumour so as to ensure assessment of the serosal aspect of the tumour, washed in cold water and then fixed in 10% neutral buffered formalin for at least 48 hours at room temperature. Representative tissue blocks were embedded in wax and sections were then stained with haematoxylin and eosin for histopathological diagnosis. Areas of tissue to be sampled were first identified and marked on the appropriate haematoxylin and eosin stained slide by GIM, an expert gastro-intestinal pathologist.

##### **Immunohistochemistry-multi-tissue and colorectal microarrays**

To dewax the tissue microarrays slides, they were immersed in xylene for 10 minutes. The slides were then rehydrated by immersion for 2 minutes in decreasing ethanol concentrations. Antigen retrieval was performed by heating the sections in a microwave (800W) for 20 minutes while they are fully immersed in citrate buffer (pH=6). The slides were allowed to cool off and then were incubated for 60 minutes at room temperature with primary antibody (culture supernatants). All primary antibodies were used undiluted except for ELOVL3 which was diluted at 1:10 in antibody diluent (Dako). Then, the sections were

washed twice with washing buffer (Dako) and blocked with peroxidase blocking solution (Dako) for 7 minutes. This was followed by further two washes with washing buffer (Dako). Peroxidase-polymer labelled goat anti-mouse secondary antibody (Envision™, Dako) was then applied for 30 minutes at room temperature. Thereafter, the slides were washed twice with Dako buffer and diaminobenzidine substrate was applied for 7 minutes to reveal sites of peroxidase activity. Finally, the sections were washed in water, immersed in copper sulphate for 2 minutes counterstained with haematoxylin for 10 seconds, and placed in Scott's tap water substitute for 2 minutes. Before being mounted, the tissue sections were dehydrated by immersion in increasing ethanol concentrations and xylene. As a negative control, antibody diluent was used to replace the primary monoclonal antibody.

### **Data analysis and statistics**

Biomarker targets were first assessed in the discovery cohort by univariate analysis using the method of Kaplan-Meier to determine the predictive performance of each biomarker. To comprehensively explore the correlations between intensity of immunostaining and survival, the expression of each protein was dichotomised into the following categories:

- Overall: negative vs weak vs moderate vs strong
- Negative vs positive i.e. negative vs weak, moderate or strong
- High vs low i.e. negative and weak vs moderate and strong
- Strong vs the remaining staining categories i.e. negative, weak and moderate vs strong

The following criterion were evaluated to determine the prognostic performance of each protein before they were considered suitable targets for validation; the ability to distinguish between good prognosis and poor prognosis groups (Kaplan-Meier plot), survival

variations between good and poor prognosis groups (median survival), chi-square value, p-value, hazard ratio with 95% confidence intervals, the number of patients in each prognostic group and robustness of the cut-off point. For each protein that showed significant association with survival, the above analysis was repeated in the validation cohort. Each protein that was associated with survival in univariate analysis was added to a multivariate model in the validation cohort to determine if any protein was independently prognostic. SPSS does not calculate a confidence interval if the cumulative survival of patients is more than 50%. Therefore, in those circumstances the confidence interval has been reported as undefined.

**Table S1. List of online bioinformatics tools, their functions and web addresses.**

<b>Name</b>	<b>Aim</b>	<b>Web address</b>
Basic Local Alignment Search Tool (BLAST)	Determination of the specificity of the immunogen peptide	<a href="http://web.expasy.org/blast/">(http://web.expasy.org/blast/)</a> and/or <a href="https://blast.ncbi.nlm.nih.gov/Blast.cgi">https://blast.ncbi.nlm.nih.gov/Blast.cgi</a>
B-cell epitope prediction tool	Prediction of accessible, hydrophilic, antigenic and flexible amino acid sequences	<a href="http://tools.immuneepitope.org/tools/bcell/iedb_input">http://tools.immuneepitope.org/tools/bcell/iedb_input</a>
PHYRE2 Protein Fold Recognition Server	Prediction of the tertiary structure of proteins	<a href="http://www.sbg.bio.ic.ac.uk/phyre2/html/page.cgi?id=index">http://www.sbg.bio.ic.ac.uk/phyre2/html/page.cgi?id=index</a>
Protter	Prediction of the secondary structure of proteins	<a href="http://wlab.ethz.ch/protter/start">http://wlab.ethz.ch/protter/start</a>
Clustal Omega	Identification of regions of high amino acids diversity by multiple alignments	<a href="http://www.ebi.ac.uk/Tools/msa/clustal_o/">http://www.ebi.ac.uk/Tools/msa/clustal_o/</a>

List of online bioinformatics tools that were used for predicting amino acids sequence that is suitable as immunogen peptide.

**Table S2. Peptide sequences used as immunogens to generate monoclonal antibodies.**

	<b>Hybridoma clone</b>	<b>Peptide sequence N-terminus – C-terminus</b>	<b>Peptide location</b>
CIDEA	V62P1E3*B10	QAKGRFTCG	211-219
ELOVL3	V61 P2B3*D10	QPYNFELSK	16-24
ELOVL5	Z88	NNVKPRKLR	289-297
UCP1	Vab12 P4B12*A12	GIKPRYTGTY	149-158

**Table S3. The numbers of normal and tumour tissue samples in the multi-tissue microarray.**

Tissue type	Normal tissue (n=51)	Tumour tissue (n=68)
Breast	4	4
Oesophagus	4	4
Stomach	4	4
Colon	4	4
Liver	4	4
Pancreas	4	4
Prostate	4	4
Kidney	4	4
Bladder tumour	-	4
Lymph node/lymphoma	1	3
Sarcoma/GIST	-	8
Adrenal-normal	4	-
Thyroid	2	2
Ovary-tumour	-	4
Endometrium-tumour	-	4
Normal skin/melanoma	2	3
Lung	4	4
Testis	2	4
Placenta	4	-

The multi-tissue microarray was developed by the NHS Grampian Biorepository, Aberdeen, UK.

**Table S4. Comparison of the clinico-pathological characteristics of the discovery and validation cohorts.**

Clinico-pathological characteristic		Discovery cohort	Validation cohort	Chi-squared value: discovery vs validation
		Percentage (number)	Percentage (number)	
Gender	Male	52.9 (145)	51.9 (285)	p=0.785
	Female	47.1 (129)	48.1 (264)	
Age	<70	43.4 (119)	45.5 (249)	p=0.601
	≥70	56.6 (155)	54.6 (300)	
Bowel screening programme detected	Yes	12 (33)	9.1 (50)	p=0.187
	No	88 (241)	90.9 (499)	
Tumour site	Proximal colon	34.3 (94)	40.2 (221)	p=0.227
	Distal colon	46 (126)	40.7 (223)	
	Rectum	19.7 (54)	19.1 (105)	
Tumour differentiation	G1/G2, well/moderate	90.9 (249)	92.3 (507)	p=0.466
	G3, poor	9.1 (25)	7.7 (42)	
Extramural venous invasion	V1, present	23.4 (64)	20.4 (112)	p=0.330
	V0, absent	76.6 (210)	79.6 (437)	
Mismatch repair protein status	Deficient	23.1 (62)	12.7 (68)	<b>p&lt;0.001</b>
	Proficient	76.9 (206)	87.3 (468)	
pT category	pT1	5.8 (16)	4.5 (25)	p=0.176
	pT2	12.8 (35)	17.5 (96)	
	pT3	63.5 (174)	63.9 (351)	
	pT4	17.9 (49)	14.1 (77)	
pN category	pN0	58 (159)	58 (320)	p=0.990
	pN1	26 (70)	26 (141)	
	pN2	16 (45)	16 (88)	
UICC stage	I	16.4 (45)	18.2 (100)	p=0.802
	II	41.6 (114)	40.1 (220)	
	III	42 (115)	41.7 (229)	
Low risk vs high risk	Low risk	46.4 (127)	45.5 (250)	p=0.825
	High risk	53.6 (147)	54.5 (299)	

Significant values are highlighted in bold. Only the mismatch repair protein status was significantly different between the two cohorts

**Table S5. The relationship between clinico-pathological parameters and the expression of each protein categorised as negative *versus* weak *versus* moderate *versus* strong.**

	CIDEA				ELOVL3				UCP1			
	Discovery		Validation		Discovery		Validation		Discovery		Validation	
	$\chi^2$	p-value	$\chi^2$	p-value	$\chi^2$	p-value	$\chi^2$	p-value	$\chi^2$	p-value	$\chi^2$	p-value
Gender (male <i>vs</i> female)	4.327	0.228	6.892	0.075	10.171	<b>0.017</b>	5.222	0.156	3.558	0.313	5.029	0.170
Age (< 70 <i>vs</i> $\geq$ 70)	2.848	0.416	3.427	0.330	0.463	0.927	15.998	<b>0.001</b>	1.442	0.696	4.843	0.184
Bowel screening programme detected (no <i>vs</i> yes)	3.591	0.309	2.212	0.530	9.926	<b>0.019</b>	3.384	0.336	3.629	0.304	6.735	0.081
Tumour site												
Proximal <i>vs</i> distal <i>vs</i> rectum	6.742	0.345	2.630	0.854	3.818	0.701	3.188	0.785	11.249	0.081	4.921	0.554
Colon <i>vs</i> rectum	4.039	0.257	0.154	0.985	2.390	0.495	1.776	0.620	9.357	<b>0.025</b>	2.881	0.410
Mismatch repair protein status (deficient <i>vs</i> proficient)	16.453	<b>0.001</b>	4.128	0.248	16.143	<b>0.001</b>	20.290	<b>&lt;0.001</b>	14.658	<b>0.002</b>	3.649	0.302
Tumour differentiation (well/moderate <i>vs</i> poor)	5.674	0.129	1.190	0.755	15.936	<b>0.001</b>	1.171	0.760	4.390	0.222	2.748	0.432
Extramural venous invasion (present <i>vs</i> absent)	7.874	<b>0.049</b>	3.474	0.324	7.909	<b>0.048</b>	10.859	<b>0.013</b>	5.000	0.172	3.952	0.267
Tumour category (pT1 <i>vs</i> pT2 <i>vs</i> pT3 <i>vs</i> pT4)	15.270	0.084	18.408	<b>0.031</b>	12.806	0.172	17.792	<b>0.038</b>	18.989	<b>0.025</b>	18.180	<b>0.033</b>
Lymph node category (pN0 <i>vs</i> pN1 <i>vs</i> pN2)	16.910	<b>0.010</b>	17.191	<b>0.009</b>	17.709	<b>0.007</b>	2.966	0.813	24.282	<b>&lt;0.001</b>	24.822	<b>&lt;0.001</b>
UICC stage (I <i>vs</i> II <i>vs</i> III)	10.152	0.118	25.073	<b>&lt;0.001</b>	15.669	<b>0.016</b>	14.546	<b>0.024</b>	32.882	<b>&lt;0.001</b>	30.550	<b>&lt;0.001</b>
Low risk <i>vs</i> high risk	6.460	0.091	15.496	<b>0.001</b>	10.957	<b>0.012</b>	5.939	0.115	18.744	<b>&lt;0.001</b>	9.921	<b>0.019</b>

Chi-squared test. Significant values are highlighted in bold. ELOVL5 was not included as there were significant differences in its expression profile between the discovery and validation cohorts.



**Table S6. The relationship between pathological parameters and the expression of UCP1 when it was categorised as either negative or positive in each cohort.**

	Discovery		Validation	
	$\chi^2$	p-value	$\chi^2$	p-value
Gender (male <i>vs</i> female)	3.385	0.066	2.791	0.095
Age (< 70 <i>vs</i> $\geq$ 70)	0.704	0.401	2.133	0.144
Bowel screening programme detected (no <i>vs</i> yes)	0.577	0.448	0.430	0.512
Tumour site				
Proximal colon <i>vs</i> distal colon <i>vs</i> rectum	6.319	<b>0.042</b>	2.439	0.295
Colon <i>vs</i> rectum	4.832	<b>0.028</b>	2.350	0.125
Mismatch repair protein status (deficient <i>vs</i> proficient)	14.406	<b>&lt;0.001</b>	1.737	0.187
Tumour differentiation (well/moderate <i>vs</i> poor)	3.667	0.056	0.001	0.979
Extramural venous invasion (present <i>vs</i> absent)	1.677	0.195	1.511	0.219
Tumour category (pT1 <i>vs</i> pT2 <i>vs</i> pT3 <i>vs</i> pT4)	7.582	0.055	14.203	<b>0.003</b>
Lymph node category (pN0 <i>vs</i> pN1 <i>vs</i> pN2)	18.199	<b>&lt;0.001</b>	14.325	<b>0.001</b>
UICC stage (I <i>vs</i> II <i>vs</i> III)	19.185	<b>&lt;0.001</b>	19.659	<b>&lt;0.001</b>
Low risk <i>vs</i> high risk	12.533	<b>&lt;0.001</b>	6.594	<b>0.010</b>

Chi-squared test, significant values are highlighted in bold.

**Table S7. Multivariate analysis of age, tumour differentiation, EMVI, tumour stage, lymph node stage and UCP1 in the validation cohort.**

Variable		Number of deaths/number of patients	Wald value	p-value	Hazard ratio (95%CI)
Age at surgery (< 70* vs ≥ 70)	< 70 ≥ 70	79/249 150/300	33.143	<b>&lt;0.001</b>	2.380 (1.772-3.197)
Tumour differentiation (well/moderate* vs poor)	Poor Well/moderate	19/42 210/507	1.973	0.160	0.664 (0.375-1.176)
Extramural venous invasion (present vs absent*)	Absent Present	152/437 77/112	17.749	<b>&lt;0.001</b>	1.959 (1.443-2.679)
Tumour category (pT1 vs pT2*) (pT2 vs pT3*) (pT3 vs pT4*)	pT1 pT2 pT3 pT4	9/25 27/96 149/351 44/77	0.979 6.245 5.503	0.323 <b>0.012</b> <b>0.019</b>	0.669 (0.302-1.483) 0.509 (0.300-0.864) 0.644 (0.446-0.930)
Lymph node category (pN0 vs pN1*) (pN1 vs pN2*)	pN0 pN1 pN2	97/320 71/141 61/88	41.004 6.969	<b>&lt;0.001</b> <b>0.008</b>	0.293 (0.202-0.427) 0.600 (0.410-0.877)
UCP1 (negative* vs positive)	Negative Positive	101/214 112/303	5.059	<b>0.024</b>	0.724 (0.546-0.959)

Significant values are highlighted in bold. \*represents the reference group.

**Table S8. Multivariate analysis of UCP1 using parameters that would be available with a biopsy in the validation cohort.**

Variable		Number of deaths/number of patients	Wald value	p-value	Hazard ratio (95%CI)
Age (< 70* vs ≥ 70)	< 70	79/249	20.205	<b>&lt;0.001</b>	1.996 (1.477-2.698)
	≥ 70	150/300			
Gender (male* vs female)	Male	118/285	0.000	0.991	0.998 (0.758-1.316)
	Female	111/264			
Bowel screening programme detected (no vs yes*)	No	220/499	1.372	0.241	1.510 (0.758-3.011)
	Yes	9/50			
Tumour site (colon vs rectum*)	Colon	177/444	0.567	0.451	0.881 (0.633-1.226)
	Rectum	52/105			
Mismatch repair protein status (proficient* vs deficient)	Proficient	188/468	1.614	0.204	1.289 (0.871-1.906)
	Deficient	33/68			
Tumour differentiation (well/moderate* vs poor)	Poor	19/42	0.946	0.331	0.745 (0.411-1.348)
	Well/moderate	210/507			
UCP1 (negative* vs positive)	Negative	101/214	11.779	<b>0.001</b>	0.614 (0.464-0.811)
	Positive	112/303			

Significant values are highlighted in bold. \*represents the reference group.

**Figure S1. Sequence alignment of proteins targets and their family members completed by multiple alignment (Clustal Omega) (peptides highlighted in yellow are peptides immunogens).**

### 1.1 CIDEA

```

SP|Q96AQ7|CIDEA_HUMAN MEYAMKSLSLLYPKSLSRHVSVRTSVVTQQLLSESPKAPRARPCRSTADRSVRKGIMA 60
SP|O60543|CIDEA_HUMAN MEAA-----RDYAGALIRPLTFMGSQT-KR--VLFTPLMHPARPFVSNHDRSSRRGVMA 52
SP|Q9UHD4|CIDEA_HUMAN ----MEYLSALNPSDLLRSVSNISSEFGRR---VWTSAPPPQRPFRVCDHKRTIRKGLTA 53
          * * :: *   ::   :       ** *.  .*: *: *
SP|Q96AQ7|CIDEA_HUMAN YSLEDLLLKVRDTLMLADKPFLLVLEEDGTTVETEEYFQALAGDTVFMVLQKGQKWQPPS 120
SP|O60543|CIDEA_HUMAN SSLQELISKTLDALVIATGLVTLVLEEDGTVDTEEFFQTLGDNTHFMILEKGQKWMPGS 112
SP|Q9UHD4|CIDEA_HUMAN ATRQELLAKALETLLL-NGVLTLVLEEDGTAVDSEDFQLLEDDTCLMVLQSGQSWSPTR 112
          : ::*: * . ::*: . *****.*:~::~* * .:* :~::~*~::~* *
SP|Q96AQ7|CIDEA_HUMAN EQGTRHPLSLSHKPAKKIDVARVTFDLYKLNPKDFIGCLNVKATFYDTYSLSYDLHCCGA 180
SP|O60543|CIDEA_HUMAN QHVP-----TCSPPKRSGIARVTFDLYRLNPKDFIGCLNVKATMYEMYSVYDIRCTGL 166
SP|Q9UHD4|CIDEA_HUMAN SGVLSYGLG-RERPKHSDIARFTFDVYKQNPRLDFGSLNVKATFYGLYSMSCDFQGLGP 171
          .          * : .:~::~*~::~*~::~*~::~*~::~*~::~*~::~*~::~*~::~*~::~*~::~*~::~*
SP|Q96AQ7|CIDEA_HUMAN KRIMKEAFRWALFSMQATGHVLLGTSCYLQQLLDATEEGQPPKPKASSLIPTCLKILQ 238
SP|O60543|CIDEA_HUMAN KGLLRSLRFLSYSAQVTGQFLIYLGTYMLRVLDDKEERPSLRSQAKGRF-TCG---- 219
SP|Q9UHD4|CIDEA_HUMAN KKVLRELLRWTSTLLQGLGHMLLGISSTLRHAVEGAEQWQK-GRLHSY----- 219
          * :~::~*~::~*~::~*~::~*~::~*~::~*~::~*~::~*~::~*~::~*~::~*~::~*~::~*

```

### 1.2 ELOVL family

```

SP|A1L3X0|ELOV7_HUMAN -----MAFSDLTSRTVHLYDNWIKDADPRVEDWLLMSSPLP-QTILLGFYVYF 47
SP|Q9BW60|ELOV1_HUMAN -----MEAVVNLYQEVMKHADPRIQGYPLMGSPLL-MTSILLTYVYF 41
SP|Q9NYP7|ELOV5_HUMAN -----MEHFDAASLSTYFKALLGPRDTRVKGWFLLDNYIP-TFICSVIYLLI 45
SP|Q9NXB9|ELOV2_HUMAN -----MEHLKAFDDEINAFLDNMFGRDRSRVGRWFMLDSYLP-TFFLTVMYLLS 48
SP|Q9GZR5|ELOV4_HUMAN MGLLDSEPGSVLNVVSTALNDTVEFYRWTWSIADKRVENWPLMQSPWP-TLSISTLYLLF 59
SP|Q9H5J4|ELOV6_HUMAN -----MNMSV---LTLQEYEFKQFNEN--EAIQWMQENWKKSFLSALYAAF 43
SP|Q9HB03|ELOV3_HUMAN -----MVTAMNVSHEVNQLFQPYNFEL--SK--DMRPFEEYWATSFPIALIYLVL 47
          .          :   .          *
SP|A1L3X0|ELOV7_HUMAN VTSLGPKLMENRKPFEKAMITYNFFIVLFSVY-----MCYEFVMSGWGIGYSFRC 99
SP|Q9BW60|ELOV1_HUMAN VLSLGPRIANRKPFLRGMIVYNFSLVALSLY-----IVYEFMSGWLSTYTWRC 93
SP|Q9NYP7|ELOV5_HUMAN V-WLGPKYMRNKQPFSCRGILVVYNLGLTLLSLY-----MFCELVTVWEGKYNFFC 96
SP|Q9NXB9|ELOV2_HUMAN I-WLGNKYMKNRPAISLRGILTLYNLGITLLSAY-----MLAELILSTWEGGYNLQC 99
SP|Q9GZR5|ELOV4_HUMAN V-WLGPKWMDREPFQMRVLIIYNFGMVLLNLF-----IFRELFMGSYNAGYSYIC 110
SP|Q9H5J4|ELOV6_HUMAN I-FGGRHLMNKRAKFKELRKLPLVLSLTLAVFSIFGALRTGAYMVYILMTKGLKQ---SVC 99
SP|Q9HB03|ELOV3_HUMAN I-AVGQNYMKERKGFNLQGPLILWFSCLAIFSI LGAVRMWGMGTVLLTGGLKQ---TVC 103
          :   * . * .: .: : : :~::~*~::~*~::~*~::~*~::~*~::~*~::~*~::~*~::~*~::~*~::~*~::~*~::~*

```

```

SP|A1L3X0|ELOV7_HUMAN DIVDYSRSPTALRMARTCWLYYFSKFIELDLDTIFFVLRKKNQVTFHLVHFHHTIMPWTWW 159
SP|Q9BW60|ELOV1_HUMAN DPVDYSNSPEALRMVRVAWLFLFSKFIELDLDTVIFILRKKDGQVTFHLVHFHHSVLPWSWW 153
SP|Q9NYP7|ELOV5_HUMAN QGTRT-AGESDMKIIRVLWVYFYSKLIIEFMDTFFFILRKNNHQITVLHVYHHASMLNIWW 155
SP|Q9NXB9|ELOV2_HUMAN QDLTS-AGEADIRVAKVLWVYFYSKSVFELDTIFFVLRKKTQSITFLHVYHHASMFNIWW 158
SP|Q9GZR5|ELOV4_HUMAN QSVDYSNNVHEVRIAAALWVYFVSKGVEYLDTVFFILRKKNNQVSFLHVYHHCTMFTLWW 170
SP|Q9H5J4|ELOV6_HUMAN DQGFYNGPV----SKFWAYAFVLSKAPELGDTIFIIILRQ--KLIFLHWYHHITVLLYSW 153
SP|Q9HB03|ELOV3_HUMAN FINFIDNST----VKFWSWVFLLSKVIELGDTAFIILRKR--PLIFIHWHYHHSTVLVYTS 157
      : : .** * ** :::***. : .:* :** :
SP|A1L3X0|ELOV7_HUMAN FGVKFAAGGLGTFHALLNTAVHVVMYSYYGLSALGPAYQKYLWKKYLTSLQLVQFVIVA 219
SP|Q9BW60|ELOV1_HUMAN WGVKIAPGGMGSFHAMINSSVHVIMYLYYGLSAFGPVAQPYLWKKHMTAIQLIQFVLVS 213
SP|Q9NYP7|ELOV5_HUMAN FVMNWVPCGHSYFGATLNSFIHVLMSYYGLSSV-PSMRPYLWKKYITQGQLLQFVLT I 214
SP|Q9NXB9|ELOV2_HUMAN CVLNWIPCGQSFFGPTLNSFIHILMSYYGLSVF-PSMHKYLWKKYLTQAQLVQFVLT I 217
SP|Q9GZR5|ELOV4_HUMAN IGIKWVAGGQAFFGAQLNSFIHVIMYSYYGLTAFGPWIQKYLWKKRYLTMLQLIQFHVTI 230
SP|Q9H5J4|ELOV6_HUMAN YSYKDMVAGGGWF-MTMNMGVHVMYSYYALRAAGFRVSR--KFAMFITLSQITQMLMGC 210
SP|Q9HB03|ELOV3_HUMAN FGYKNKVPAGGWF-VTMNFGVHAIMYTYTTLKAANVKPPK--MLPMLITSLQILQMFVGA 214
      : . . * :* :* :** ** * :* * : * : :
SP|A1L3X0|ELOV7_HUMAN IHIS---QFFFMEDCKYQFPVFAC-IIMSYSFMFLLLFLHFWYRAYTKGQRLPKTV---- 271
SP|Q9BW60|ELOV1_HUMAN LHIS---QYFMSSCNYQYPVIIH-LIWMYGTIFFMFLFSNFWYHSYTKGKRLPRAL---- 265
SP|Q9NYP7|ELOV5_HUMAN IQTS---C-GVIWPCF--PLGWLYFQIGYMISLIALFTNFYIQTYNKKGASRRKDHDKD 268
SP|Q9NXB9|ELOV2_HUMAN THTM---S-AVVKPCGF--PFGCLIFQSSYMLTLVILFLNLFYVQTYRKKPMKKDMQEP- 270
SP|Q9GZR5|ELOV4_HUMAN GHTA---L-SLYTDCPF--PKWMHWALIAYAISFIFLFLNFIIRTYKEPKKPKAGKTA-- 282
SP|Q9H5J4|ELOV6_HUMAN VVNYLVFCWMQHDQCHSHFQN-IFWSSLMY-LSYLVLFCHFFFEAYIGKMRKTTKAE--- 265
SP|Q9HB03|ELOV3_HUMAN IVSILTYIWRQDQGCHTTMEH-LFWSFILY-MTYFILFAHFFCQTYIRPKVKAKTKSQ-- 270
      * * . ** .*: .:*
SP|A1L3X0|ELOV7_HUMAN -KNG-TCKNKDN----- 281
SP|Q9BW60|ELOV1_HUMAN -QQN-GAPGIKVKAN----- 279
SP|Q9NYP7|ELOV5_HUMAN HQNGSMAAVNGHTNSFSPLENNVKPRK--LRKD 299
SP|Q9NXB9|ELOV2_HUMAN --AG-KEVKNGFSKAYFTAANGVMNKK--AQ-- 296
SP|Q9GZR5|ELOV4_HUMAN -MNGISANGVSKSEKQLMIENGKKQKNGKAKGD 314
SP|Q9H5J4|ELOV6_HUMAN -----
SP|Q9HB03|ELOV3_HUMAN -----

```

### 1.3. UCP1

```

SP|O95258|UCP5_HUMAN MGIFPGIILIFLRVKFATAAVIVSGHQKSTTVSHEMSGLNWKPFVYGGGLASIVAIEFGTFP 60
SP|P55851|UCP2_HUMAN -----MVG-----FKATDVPPTATVKFLGAGTAACIADLITFP 33
SP|P25874|UCP1_HUMAN -----MGG-----LTASDVHPTLGVQLFSAGIAACLADVITFP 33
SP|P55916|UCP3_HUMAN -----MVG-----LKPSDVPPTMAVKFLGAGTAACFADLVITFP 33
SP|O95847|UCP4_HUMAN -----MSVP-EEEEERLLPLTQRWPRASKFLLSGCAATVAELATFP 39
      : :. .* *: .*: .***

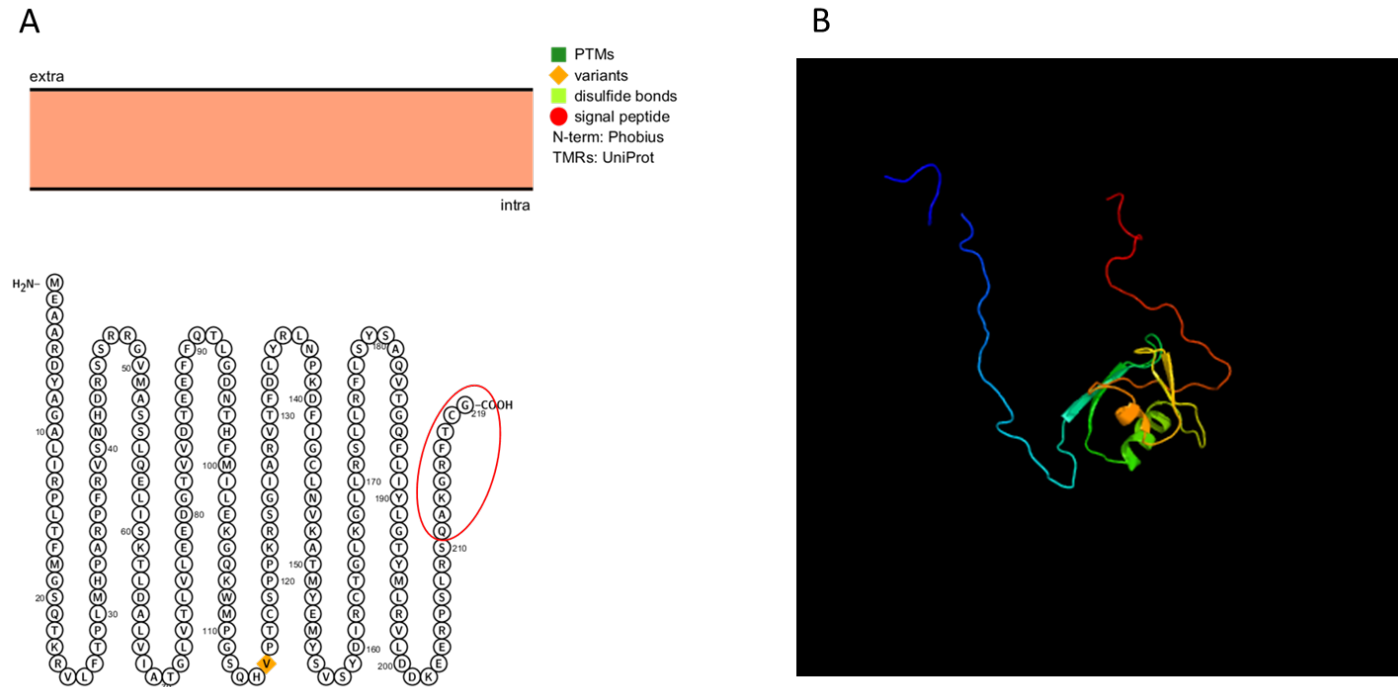
```

```

SP|095258|UCP5_HUMAN  VDLTkTRLQVQGSIDARF-----KEIKYRGMFHALFRICKEEGLVLAlySGIAPALLRQA 115
SP|P55851|UCP2_HUMAN  LDTAKVRLQIQGESQGPVR---ATASAQYRGVMGTILTMVRTEGPRSLYNGLVAGLQRQM 90
SP|P25874|UCP1_HUMAN  LDTAKVRLQVQGECP-----TSSVIRYKGVLTITAVVKTEGRMKLYSGLPAGLQRQI 86
SP|P55916|UCP3_HUMAN  LDTAKVRLQIQGENQAV-Q---TARLVQYRGVLTILTMVRTEGPCSPYNGLVAGLQRQM 89
SP|095847|UCP4_HUMAN  LDLTkTRLQMQGEAALARLGDGAREsAPYRGMVRTALGIIEEEGFLKLWQGVTPAIYRHV 99
:* :*.***:**:      *:*: : : . ** :.*: .: *:
SP|095258|UCP5_HUMAN  SYGTIKIGIYQSLKRLFVERLEDET--LLINMICGVVSGVISSTIANPTDVLKIRMQAQG 173
SP|P55851|UCP2_HUMAN  SFASVRIGLYDSVKQFYT-KGSEH-ASIGSRLLAGSTTGALAVAVAQPTDVVKVRFQAQA 148
SP|P25874|UCP1_HUMAN  SSASLRIGLYDTVQEFLLTAGKETA-PSLGSKILAGLTTGGVAVFIGQPTEVVKVRLQAQS 145
SP|P55916|UCP3_HUMAN  SFASIRIGLYDSVKQVYTPKGADN-SSLTTRILAGCTTGAMAVTCAQPTDVVKVRFQASI 148
SP|095847|UCP4_HUMAN  VYSGGRMVTYEHLREVVFVGKSEDEHYPLWKSvIGGMMAGVIGQFLANPTDLVKVQMMEG 159
. :. * :... : :. * :* :. :***::*::* .
SP|095258|UCP5_HUMAN  SLFQ-----GSMIGSFIDIYQQEGTRGLWRGVVPTAQRAAIvVGVELPVYDITKKHLI 226
SP|P55851|UCP2_HUMAN  RAGG---GRRYQSTVNAYKTIAREEGFRGLWKGTSPNVARNAIvNCAELVTYDLIKDALL 205
SP|P25874|UCP1_HUMAN  HLHGI--KPRYTGTYNAYRIIATTEGLTGLWKGTTPNLmRSVIINCTELVTYDLMKEAFV 203
SP|P55916|UCP3_HUMAN  HLGPSRSDRKYSGTMDAYRTIAREEGVRGLWKGTLPNIMRNAIvNCAEVVTYDILKEKLL 208
SP|095847|UCP4_HUMAN  KRKLEGKPLRFRGVHHAFAKILAEGGIRGLWAGWVPNIQRAALvNMGLTtTYDtvKHylV 219
. :. * : * * * * * . * :. :. :. ** * . :.
SP|095258|UCP5_HUMAN  LSGMMGDTILTHFVSSFTcGLAGALASNPVDVVRTRMMNQR-AIVGHVDLYKGTVDGILK 285
SP|P55851|UCP2_HUMAN  KANLMTDDLPCHFtSAFGAGFCTTVIASPVDVVKTRYMNSAL-----GQYSSAGHCALT 259
SP|P25874|UCP1_HUMAN  KNNILADDVPCHLVsALIAGFCATAMSSPVDVVKTRFINSPP-----GQYKsvPNCAMK 257
SP|P55916|UCP3_HUMAN  DYHLLTDNFPCHFvSAFGAGFCATVVASPVDVVKTRYMNSPP-----GQYFSPLDCMIK 262
SP|095847|UCP4_HUMAN  LNTPLEDNIMTHGLSSLCsGLVASILGTPADVIKSRIMNQPRDKQGRGLLYKSSTDCLIQ 279
: * . * *::.*: : ..*.*:::* :*. * . . :
SP|095258|UCP5_HUMAN  MWKHEGFFALYKGFwPNWLRlGPWNIIFFITyEQlKRLQI----- 325
SP|P55851|UCP2_HUMAN  MLQKEGPRAFYKGFmPSFLRLGSWNvVMFVtYEQlKRALMAACTSREAPF 309
SP|P25874|UCP1_HUMAN  VFTNEGPTAFFKGLVPSFLRLGSWNvIMFVCFEQlKRELSKSRQTMDCAT 307
SP|P55916|UCP3_HUMAN  MVAQEGPTAFYKGFtPSFLRLGSWNvVMFVtYEQlKRALMKVQMLRESPF 312
SP|095847|UCP4_HUMAN  AVQGEgFMSLYKGFLPswLRMTpWSMVfWLTyEKIREMSGVSPF----- 323
** :::**:* :.*::* :* :.::* :* :.

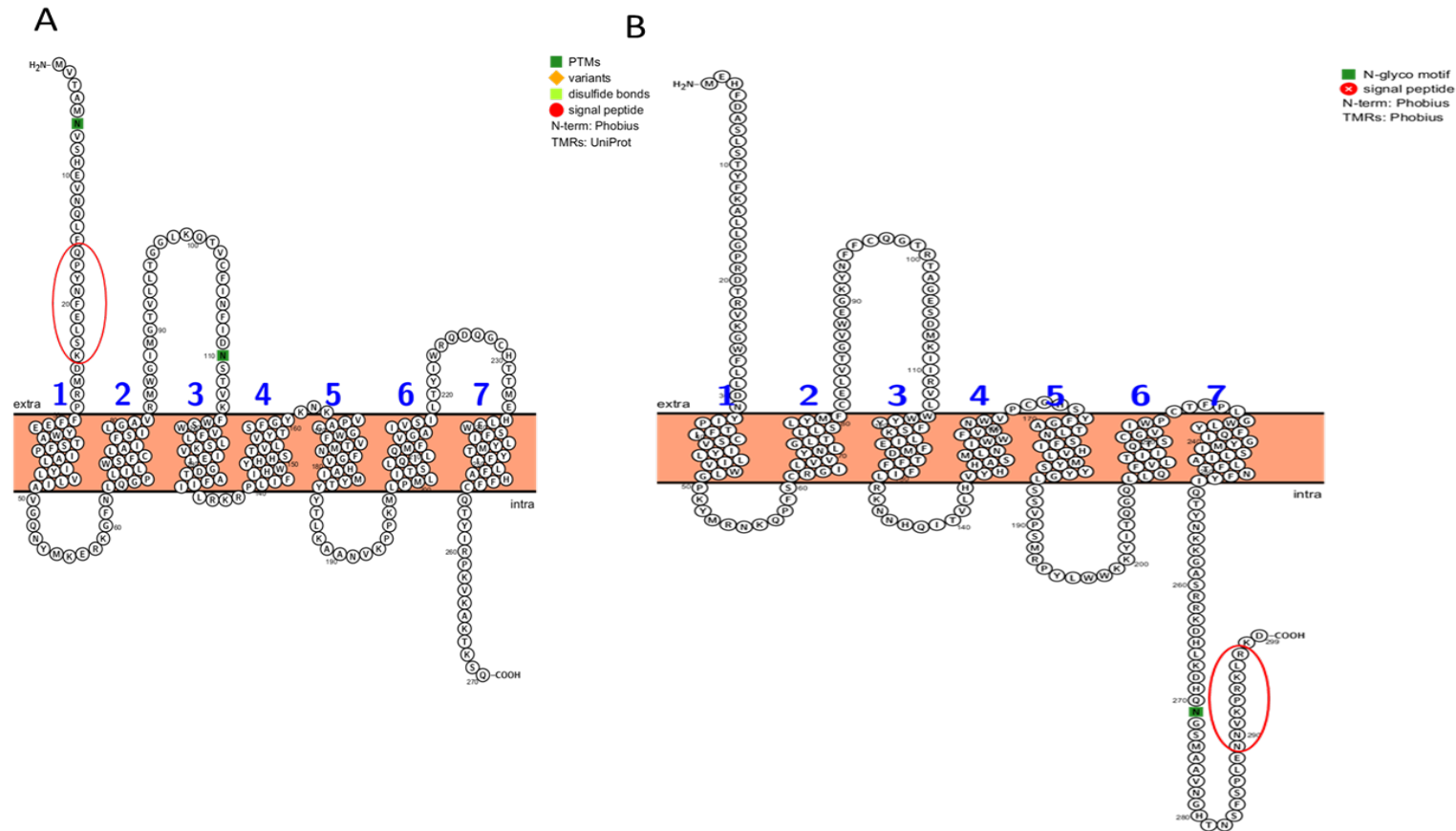
```

**Figure S2. The predicted secondary and tertiary structure of CIDEA.**



A. The secondary structure of CIDEA was predicted by Protter software.<sup>1</sup> Encircled sequence was selected for immunisation to generate anti-CIDEA antibody. B. The tertiary structure of CIDEA predicted by Protein Fold Recognition Server PHYRE2.<sup>2</sup> The tertiary structure of the region from which the peptide was selected was not predicted since only 121 residues (55% of sequence) have been modelled with 100.0% confidence). Therefore, peptide was selected from the C-terminus region which is often highly diversified and accessible.

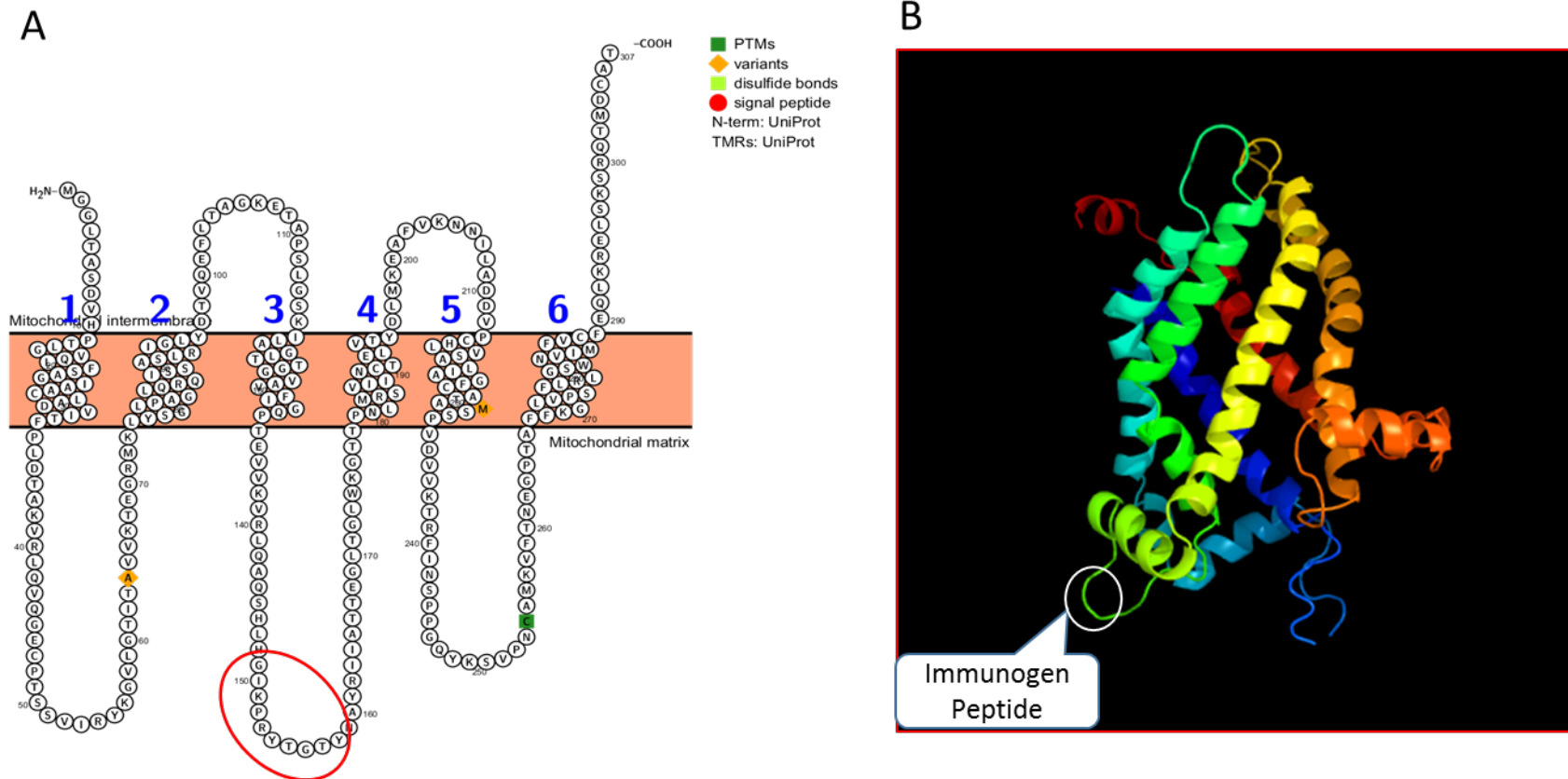
Figure S3. The predicted secondary of ELOVL3 and ELOVL5.



The secondary structures of ELOVL3 (A), ELOVL5 (B) were predicted by Protter software.<sup>1</sup> Encircled sequences were selected for immunisation to generate the corresponding antibody. The tertiary structure was not possible to predict since the prediction software could not identify regions with detectable homology to known structures. Considering there are several transmembrane regions in both enzymes, the selection of peptides was limited to the remaining regions given they are not conserved.

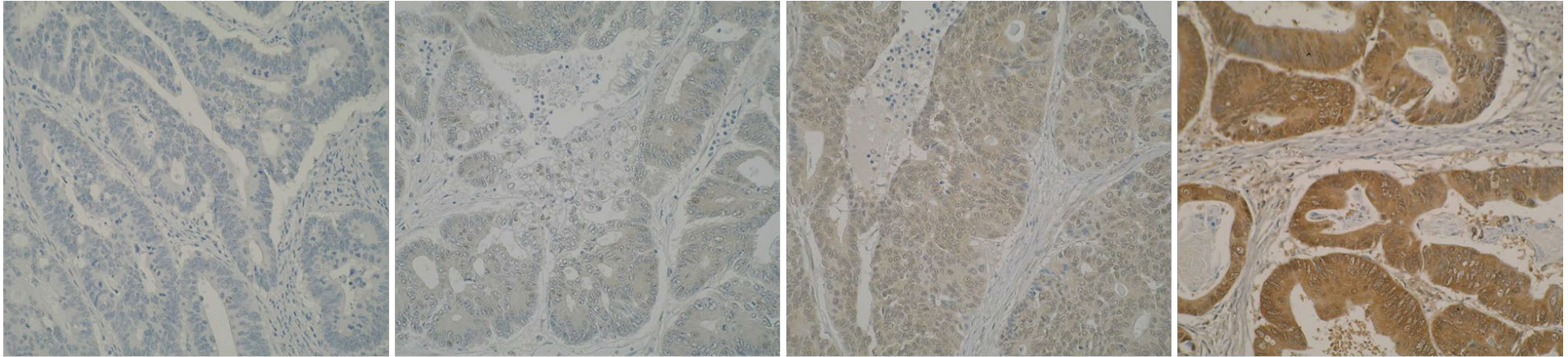


Figure S4. The predicted secondary and tertiary structure of UCP1.



A. The secondary structure of UCP1 predicted by Protter software.<sup>1</sup> Short sequence (10 amino acids) was selected for immunisation to generate anti-UCP1 antibody. B. The tertiary structure of UCP1 predicted by Protein Fold Recognition Server PHYRE2.<sup>2</sup> Colour rainbow (red to blue) mirror the protein sequence from C-terminal to N-terminal (291 residues (95% of sequence) have been modelled with 100.0% confidence). The peptide selected for anti-UCP1 antibody lies within an exposed, flexible and accessible region. The peptide sequence is commercially sensitive and is held for proprietary reasons.

**Figure S5. Photomicrographs of representative cores showing intensity scale of negative, weak, moderate and strong immunostaining of UCP1 in colorectal cancer.**



Negative

Weak

Moderate

Strong

**Figure S6. Immunoblots of CIDEA (24.6 kDa), ELOVL3 (31.5 kDa), ELVOL5 (35.2 kDa), and UCP1 (33 kDa) monoclonal antibodies.** The left-hand lane (+) of each panel contains five micrograms of cell lysate (HEK293) overexpression the relevant protein. The right-hand lane (-) of each panel contains five micrograms of empty vector transfected control cell lysate (HEK293). To overexpress each protein, HEK293 cells had been transiently transfected using full length reading frame cDNA plasmid of the corresponding target (Novus Biologicals, Oxfordshire, UK and OriGene Technologies Rockville, USA).

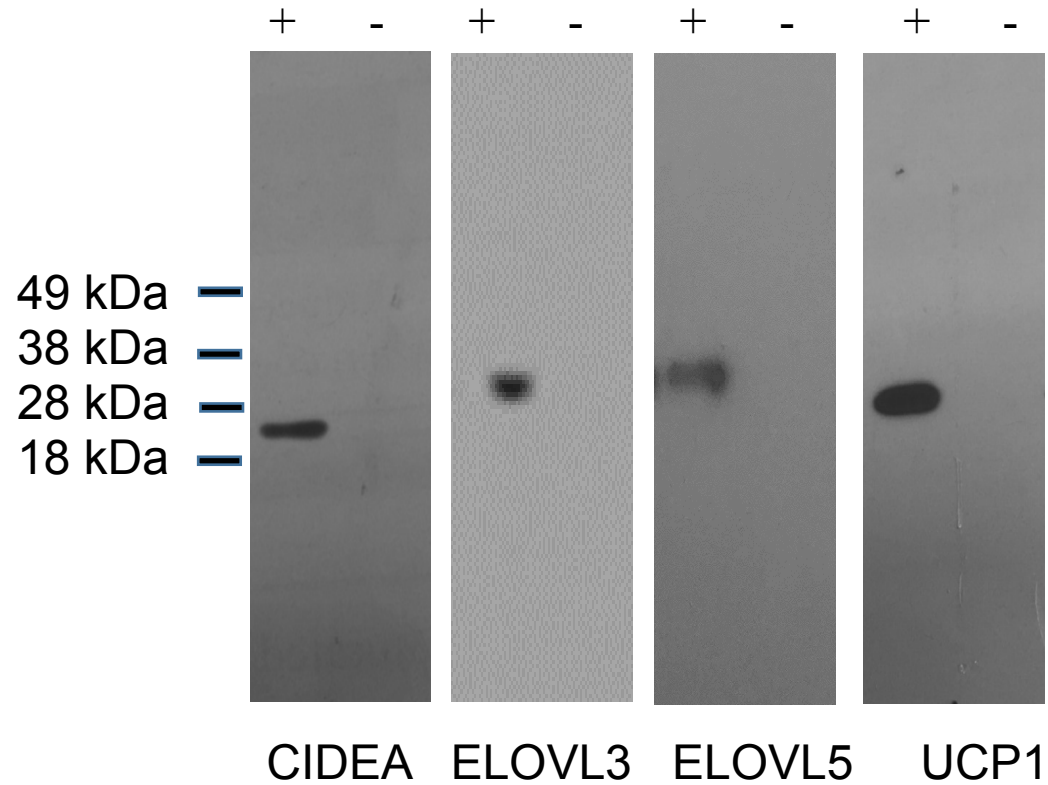
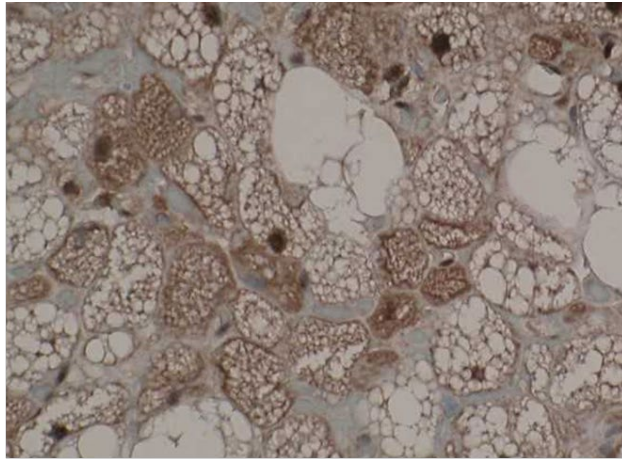
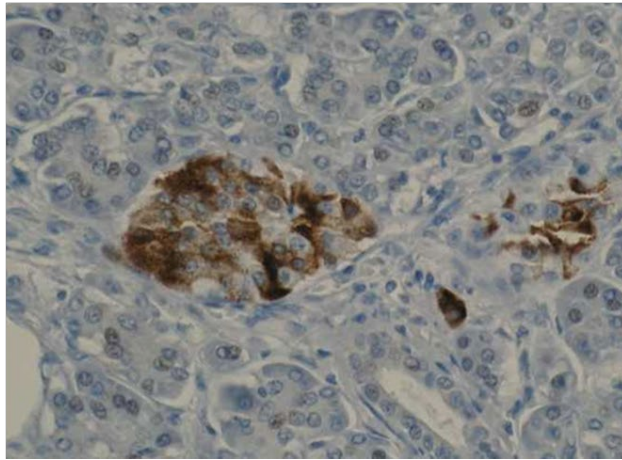


**Figure S7. Photomicrographs of UCP1 in hibernoma and endocrine pancreas**

Hibernoma



Pancreas



There is strong immunoreactivity for UCP1 in hibernoma (brown fat tumour) and the islets of Langerhans of the pancreas (endocrine pancreas).

**Figure S8. Photomicrographs of CIDEA, ELOVL3, ELOVL5 and UCP1 in normal colonic mucosa and primary colorectal cancer.**

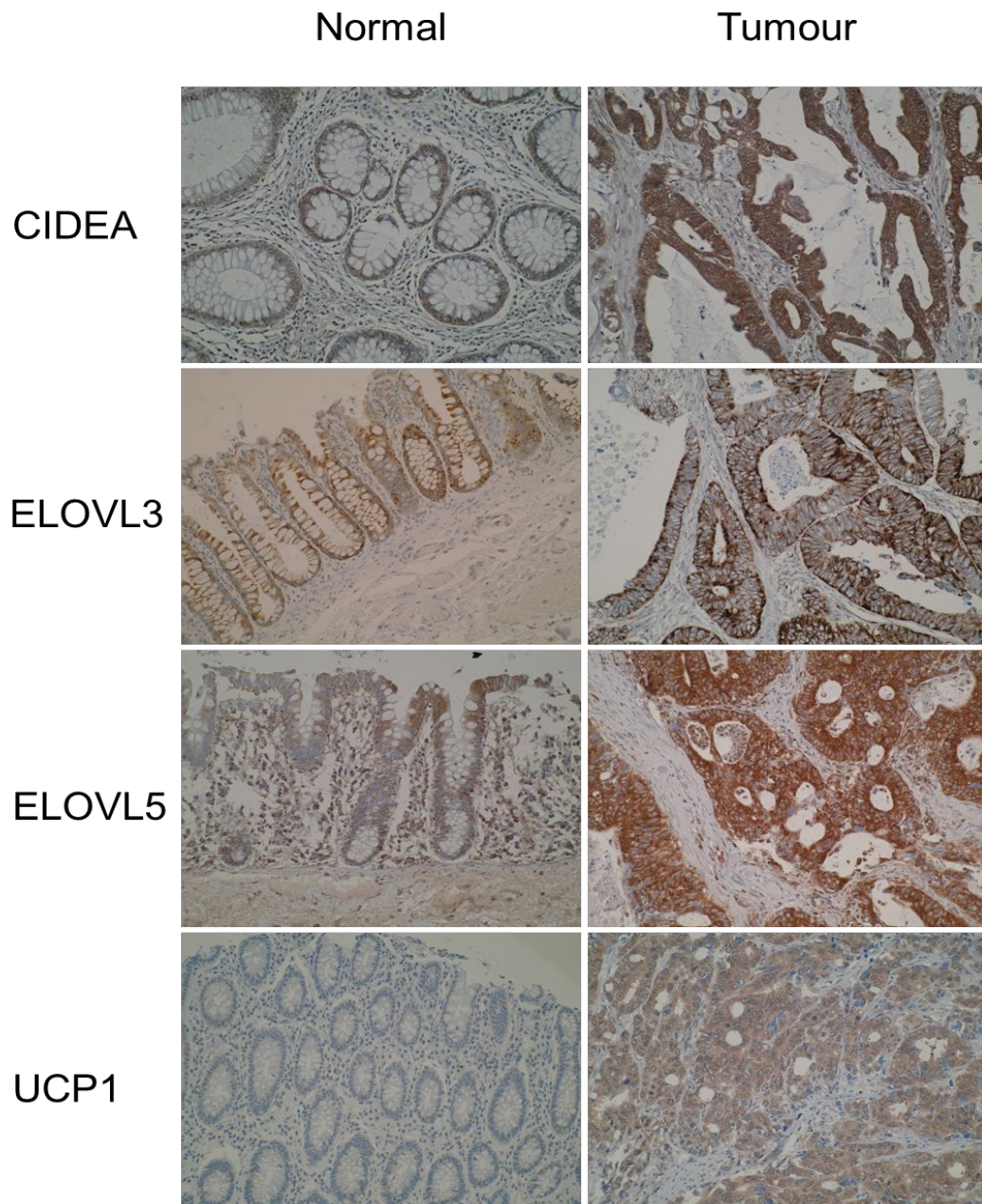


**Figure S9.** The frequency of positive and negative immunostaining of UCP1 in individual colorectal cancer stages (stage I vs stage II vs stage III) in the discovery and validation cohorts.

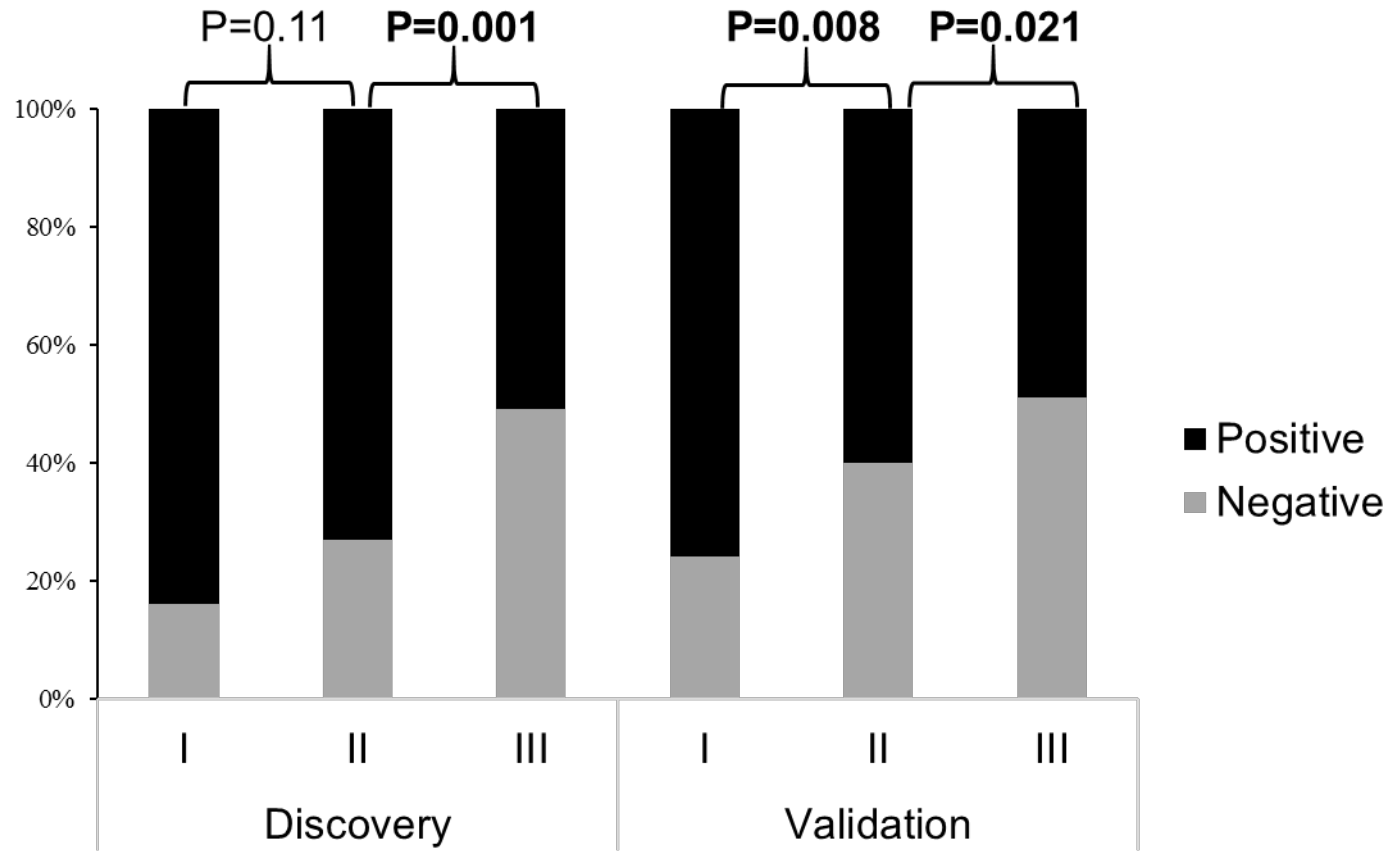


**Figure S10. The relationship between the expression of CIDEA categorised as negative vs positive, and survival in the discovery cohort (A) and in the validation cohort (B).**

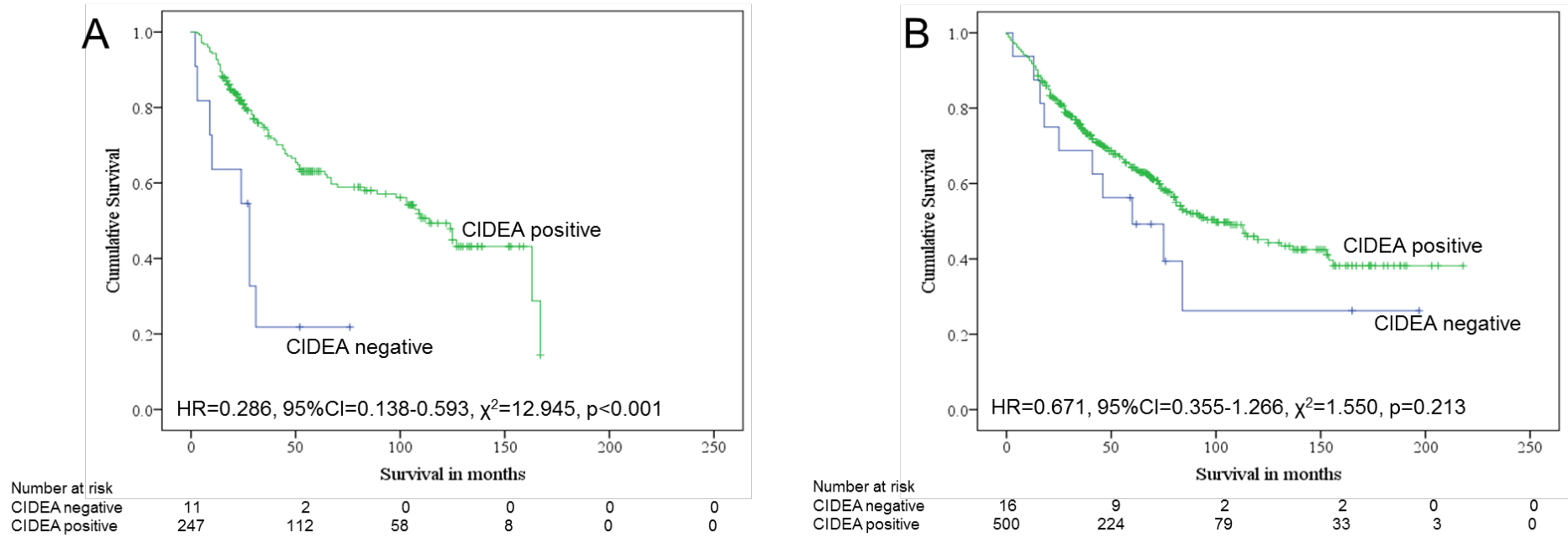
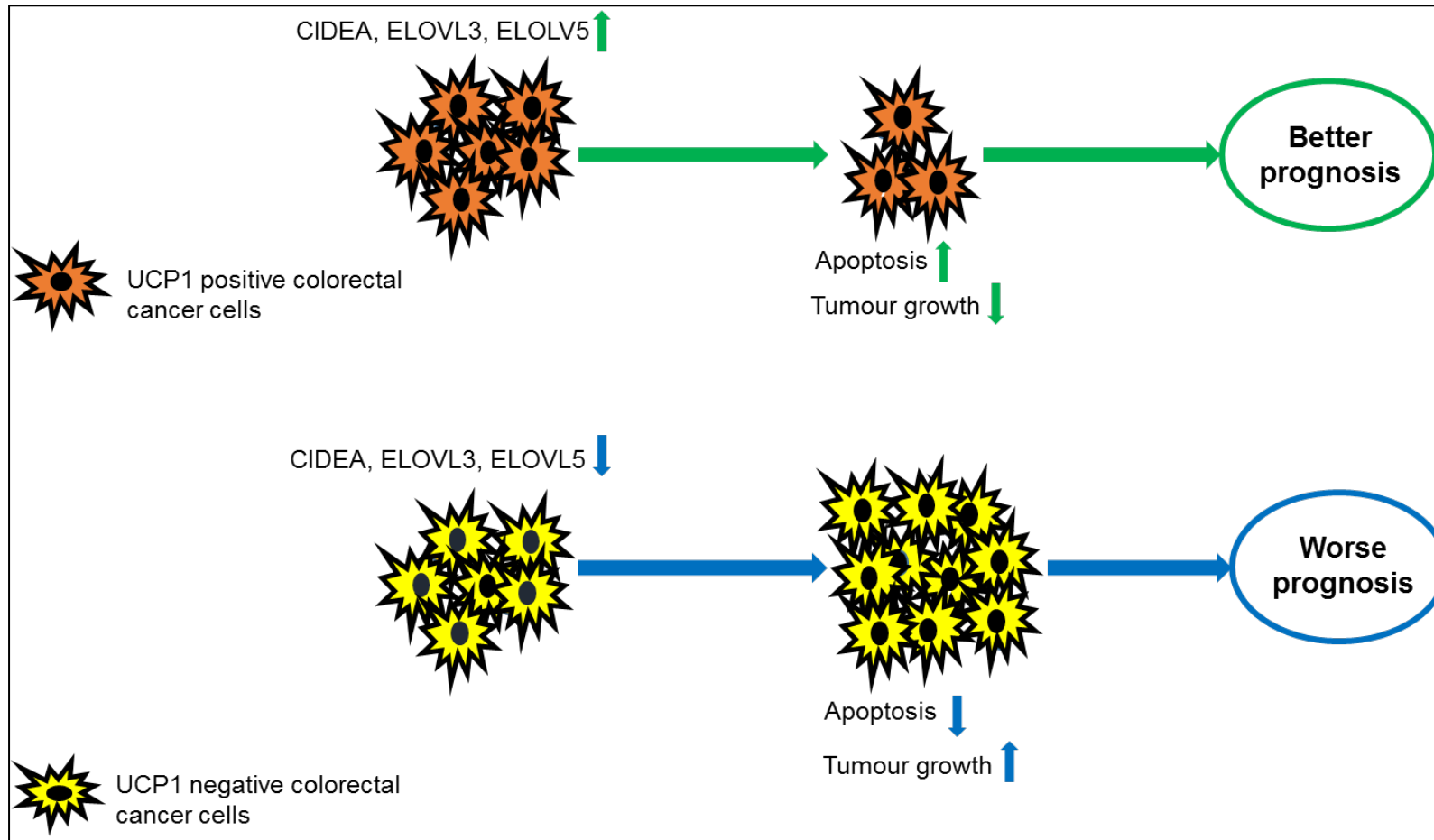


**Figure S11. A schematic pathway demonstrating the impact of UCP1 expression in colorectal cancer.** The expression of UCP1 in the epithelial compartment of colorectal carcinoma inhibits tumour growth and increases apoptosis. This is translated into better prognosis compared to UCP1-negative tumours.





## References

1. Omasits U, Ahrens CH, Muller S, Wollscheid B. Protter: Interactive protein feature visualization and integration with experimental proteomic data. *Bioinformatics* 2014; **30**: 884-886.
2. Kelley LA, Mezulis S, Yates CM, Wass MN, Sternberg MJ. The Phyre2 web portal for protein modeling, prediction and analysis. *Nat Protoc* 2015; **10**: 845-858.